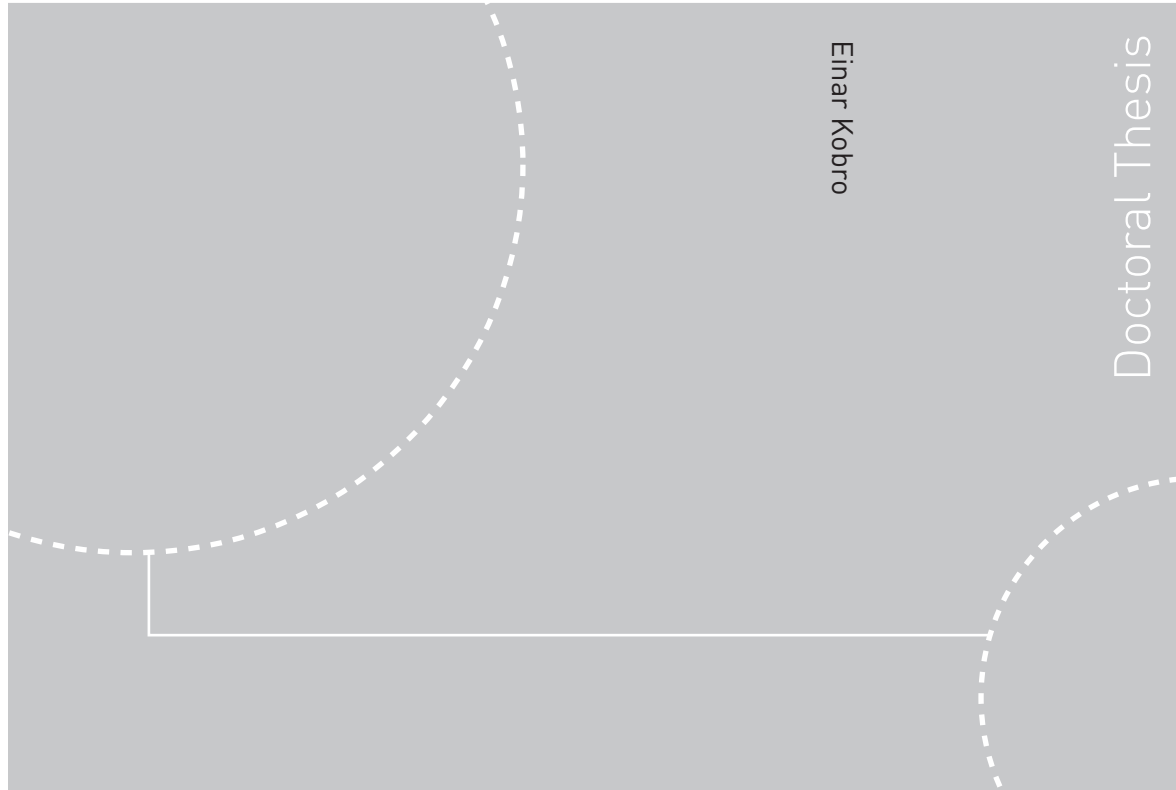


Doctoral theses at NTNU, 2010:13=

Einar Kobro

# Measurement of Pressure Pulsations in Francis Turbines



ISBN 978-82-471-2239-6 (printed ver.)  
ISBN 978-82-471-2240-2 (electronic ver.)  
ISSN 1503-8181

Doctoral theses at NTNU, 2010:137

**NTNU**  
Norwegian University of  
Science and Technology  
Thesis for the degree of  
doctor philosophiae  
Faculty of Engineering Science and Technology  
Department of Energy and Process Engineering

 **NTNU**  
Norwegian University of  
Science and Technology

 **NTNU**

 **NTNU**  
Norwegian University of  
Science and Technology

Einar Kobro

# Measurement of Pressure Pulsations in Francis Turbines

Thesis for the degree of doctor philosophiae

Trondheim, November 2010

Norwegian University of  
Science and Technology  
Faculty of Engineering Science and Technology  
Department of Energy and Process Engineering



**NTNU**

Norwegian University of  
Science and Technology

**NTNU**

Norwegian University of Science and Technology

Thesis for the degree of doctor philosophiae

Faculty of Engineering Science and Technology  
Department of Energy and Process Engineering

©Einar Kobra

ISBN 978-82-471-2239-6 (printed ver.)

ISBN 978-82-471-2240-2 (electronic ver.)

ISSN 1503-8181

Doctoral Theses at NTNU, 2010:137

Printed by Tapir Uttrykk

Einar Kobro

# Measurement of Pressure Pulsations in Francis Turbines

Thesis for the degree of philosophiae doctor

Trondheim, November 2010

Norwegian University of Science and Technology

Faculty of Engineering Science and Technology

Department of Energy and Process Engineering

Waterpower Laboratory



**NTNU**  
**Norwegian University of  
Science and Technology**

---

## **Abstract**

The work presented in this thesis involves preparation and execution of measurements on Francis runners. The measurements were performed by means of onboard measuring equipment both in model runners and full-scale prototype runners. Also, analysis of the measured data, and the discussion of the results, is presented.

The measurements resulted in large data sets. These data sets were used by the author to investigate the dynamic pressure and strain in the runners. The results of the analysis can be used as input in future turbine design. Andritz Hydro AG has used the data for verification of their numerical simulation tools.

In connection with the refurbishment of Tokke power plant, two model runners were made available for onboard pressure measurements. To investigate the dynamic pressure in these runners, methods for integration of pressure transducers in the runner blades needed to be developed. After initial difficulties during the preparation, successful measurements were obtained from both model runners.

At Tokke power plant, both the original and replacement runners were made accessible for onboard pressure and strain gauge measurements. On the original Kvaerner Brug AS runner, the test was prepared and performed by the author. This test failed, due to water intrusion in the logging chain. The second test was performed on the Andritz Hydro AG replacement runner. This test was prepared and performed by the author in close cooperation with Andritz Hydro AG, and the results were successful.

The analysis results from both model and prototype runners show that the wake leaving the guide vanes is the most severe source of dynamic pressure in the runner. The draft tube vortex rope pulsation propagates upstream the runner, but does not appear as a significant frequency in the runner strain measurements.

## Acknowledgements

During my Master thesis and PhD thesis, I have been so lucky to be a part of the Waterpower Laboratory community. This “family” has contributed with an academic and social frame that has made these years very joyful.

I would like to express my gratitude to the following:

- My two supervisors, Professor Ole Gunnar Dahlhaug and Professor Torbjørn K. Nielsen. Without their positive and co-operative approach, and very informal style, this thesis would be very different.
- Most of the work has been done in parallel with my fellow PhD candidates Håkon Hjort Francke, Jørgen Ramdal and Pål-Tore Storli. Technical discussions and social activities with you guys have been one of the important factors for why I’ve enjoyed these years so much.
- The laboratory personnel Joar Grilstad, Trygve Opland and Halvor Haukvik, who have contributed with invaluable laboratory assistance.
- EnergiNorge for funding, as well as the positive and benevolent national hydropower industry.
- Statkraft by Kjell-Tore Fjærvold, Erik J. Wiborg and the Statkraft Region Øst staff. Without their financial, administrative and practical support, this study would not have been possible.
- Andritz Hydro AG, by Alphonse Gamboa, Reinhard Bloch, and Pål Teppan, for an excellent cooperation, financial contribution and access to their runners.
- Norconsult by Halvard Bjørndal, amongst others for access to all their recorded dynamic pressure measurement data.
- Andreas, my best friend, for all that fun we’ve had since we were kids, your out-of-the-box ideas, all of our trips and adventures and your joyful attitude towards life.
- My family, for always supporting my choices. Mom, Dad and my late Grandpa, this thesis is to you.



---

**Einar Kobro**

20.06.2010, Trondheim

---

# Table of Contents

<b>ABSTRACT .....</b>	<b>III</b>
<b>ACKNOWLEDGEMENTS .....</b>	<b>IV</b>
<b>TABLE OF CONTENTS.....</b>	<b>V</b>
<b>LIST OF FIGURES .....</b>	<b>VII</b>
<b>ABBREVIATIONS.....</b>	<b>VIII</b>
<b>NOMENCLATURE.....</b>	<b>IX</b>
<b>PART 1 - SUPERSTRUCTURE .....</b>	<b>1</b>
<b>1 INTRODUCTION.....</b>	<b>3</b>
1.1 STRUCTURE OF THESIS.....	3
1.2 BACKGROUND .....	4
1.3 MOTIVATION .....	4
1.4 OBJECTIVES AND SCOPE .....	5
1.5 PREVIOUS WORK.....	6
<b>2 THEORETICAL BACKGROUND.....</b>	<b>11</b>
2.1 SOURCES OF PRESSURE PULSATIONS .....	13
2.2 MEASUREMENT EQUIPMENT BACKGROUND .....	20
2.3 ANALYZING TECHNIQUES .....	23
<b>3 MEASUREMENTS .....</b>	<b>29</b>
3.1 MODEL MEASUREMENTS .....	29
3.2 PROTOTYPE MEASUREMENTS.....	30
<b>4 SUMMARY OF PAPERS .....</b>	<b>33</b>
4.1 PAPER 1.....	33
4.2 PAPER 2.....	35
4.3 PAPER 3.....	37
4.4 PAPER 4.....	39
<b>5 GENERAL DISCUSSION .....</b>	<b>41</b>
5.1 DATA ACQUISITION HARDWARE.....	41
5.2 MEASUREMENT RESULTS .....	42



---

<b>6</b>	<b>CONCLUSION.....</b>	<b>49</b>
<b>7</b>	<b>FURTHER WORK.....</b>	<b>51</b>
7.1	PRESSURE SCALE UP, AND PRESSURE-STRAIN CORRELATION .....	51
7.2	COMPARISON OF CONVENTIONAL AND SPLITTER BLADE DESIGN.....	52
7.3	STRAIN MEASUREMENT ANALYSIS .....	52
<b>8</b>	<b>BIBLIOGRAPHY.....</b>	<b>55</b>
<b>9</b>	<b>APPENDICES .....</b>	<b>63</b>
9.1	APPENDIX 1 - SUMMARY OF PAPER 5 .....	63
9.2	APPENDIX 2 - A BRIEF DISCUSSION ON HIGH CYCLE FATIGUE.....	64
9.3	APPENDIX 3 - THE MODEL TEST RIG .....	68
9.4	APPENDIX 4 - PICTURES OF THE DRAFT TUBE VORTEX .....	70
	<b>PART 2 - PAPERS.....</b>	<b>75</b>

#### **PAPER 1**

Onboard Pressure Measurements in Francis Model Runner Blades

#### **PAPER 2**

Onboard Pressure Measurement in High Head Francis Prototype Runners

#### **PAPER 3**

Data Analysis from Onboard Francis Model Runner Pressure Measurements

#### **PAPER 4**

Analysis of Onboard Pressure and Strain Measurement Data from High Head Francis Prototype Runner, and Discussion on Runner Lifetime

## List of figures

Figure 2-1. Hill chart for the NTNU model runner .....	11
Figure 2-2. A view of the Francis turbine.....	13
Figure 2-3. Flow field at inlet of runner .....	15
Figure 2-4. Blade passing pulse .....	16
Figure 2-5. Guide vane wake travelling through runner.....	17
Figure 2-6. von Kármán vortex shedding .....	20
Figure 2-7. Folding diagram. ....	27
Figure 3-1. Parts of the Tokke regulation area. ....	31
Figure 5-1. RSI frequency amplitude, pressure side.....	45
Figure 5-2. RSI frequency amplitude, suction side .....	45
Figure 5-3. Runner channel with sensor radii .....	47
Figure 9-1. Schematic example of classical Wöhler curve .....	64
Figure 9-2. S/N curve for 17-4PH martensitic stainless steel.....	65
Figure 9-3. S/N curve for 1Cr-0.5Mo steel.....	66
Figure 9-4. Francis test rig .....	68
Figure 9-5. Cross section of the model turbine.....	69
Figure 9-6. Extreme part load .....	70
Figure 9-7. Part load.....	71
Figure 9-8. Overload .....	72
Figure 9-9. Extreme over load.....	73

## Abbreviations

BEP	Best Efficiency Point
CFD	Computational Fluid Dynamics
DFT	Discret Fourier Transform
EPFL	Ecole Polytechnique Fédéral de Lausanne
FEM/FEA	Finite Element Method / Analysis
FFT	Fast Fourier Transform
FSC	Fluid Structure Coupling
LDA	Laser Doppler Anemometry
NTNU	Norwegian University of Science and Technology
RSI	Rotor Stator Interaction
STD	Standard Deviation

## Nomenclature

Symbols	Description	Denomination
$\Omega$	Speed number	-
$\omega$	Runner rotation frequency	revolutions/s
$\sigma$	Sigma, plant submergence	-
$\Delta t$	Time step	s
$f_n$	Runner rotation frequency	Hz
$f_s$	Logging frequency	Hz
$f_N$	Nyquist of folding frequency	Hz
$f_{bp}$	Blade passing frequency	Hz
$f_{gv}$	Guide vane frequency	Hz
$f_R$	Reingans Frequency	Hz
H	Head	mWc
H*	Rated head	mWc
n	Runner rotation speed	revolutions/m
$n_{ED}$	Speed factor	-
$n_s$	Specific speed	-
P	Power	MW
Q	Flow	m <sup>3</sup> /s
Q*	Rated flow	m <sup>3</sup> /s
$q_{ED}$	Flow factor	-
Re	Reynolds number, inertial to viscous forces	-
$Z_{cf}$	Common factor between $Z_r$ and $Z_s$	-
$Z_r$	Number of runner blades	-
$Z_s$	Number of stator vanes	-



## **Part 1 – Superstructure**



# 1 Introduction

## 1.1 Structure of thesis

This thesis is divided in two parts; Part 1 – Superstructure and Part 2 – Papers.

In Part 1, *Chapter 1* contains the introduction to the thesis with background, motivation, objectives and scope, and previous work.

*Chapter 2* involves the theoretical background, with description of pressure pulsation sources, measurement equipment and analyzing techniques.

*Chapter 3* describes the model and prototype measurements performed.

*Chapter 4* contains a brief summary of the four papers included in this thesis.

*Chapter 5* discusses the data acquisition set-ups used, and the measurement results.

*Chapter 6* concludes the work presented in this thesis.

*Chapter 7* proposes further work as a continuation of this thesis.

*Chapter 8* shows the bibliography of Part 1.

*Chapter 9* contains appendixes with:

- the summary of a paper not included in this thesis
- a brief discussion on a shift in the understanding of high cycle fatigue
- a description of the model test rig
- some pictures of the draft tube vortex rope

In Part 2, the 4 published papers are presented.



## 1.2 Background

As the energy matrix is changing into a larger portion of renewable energy, several properties of hydropower increase in importance. Hydropower is a well known technology with high efficiency, high reliability, and relatively low investments compared to output. Also, the regulating capacities offered by hydropower turbines and reversible pump turbines are superior to all other renewable sources of energy. These factors combined gives hydropower a vital role in the energy matrix the coming years.

As the turbine manufacturers have strived for higher efficiencies in a competitive market, new challenges have surfaced. Several large turbines have experienced runner fatigue failure after very short time of operation [1-3]. A high efficiency turbine has low solidity, and to decrease costs the unit is designed to be compact [4]. Low solidity results in thin runner blades, and reduced radial extension increases the influence of rotor stator interaction. These factors combined are thought to be the main reason for runner fatigue failure.

As the Tokke power plant was going to be refurbished, possibilities for onboard pressure and strain measurements opened up both in model and prototype runners. These possibilities were utilized by NTNU, partially in cooperation with Andritz Hydro AG.

## 1.3 Motivation

Due to the increased use of part-load and over-load operation, power companies assess the increased maintenance cost and risk of failure. At the present time, there is no way to accurately calculate these factors. Therefore, it is a desire to further investigate the dynamic pressures appearing in Francis turbine units, to be able to avoid fatigue.

Part-load and over-load draft tube surges are known to cause system instabilities. However, the nature of these surges is not fully understood, even though they have been the topic of extensive research for decades. For the fatigue problem, the surges are not thought to be a problem. The dynamic pressure and strain in the runner need attention, due to recent failures. Few onboard

pressure and strain measurements have been published, and available measurements reports from high head units are rare. When such measurements are performed, the results are often kept confidential.

Hence, when onboard dynamic pressure and strain measurement were possible in model and prototype runners, the process of designing and preparing the logging chains started. The goal of the work presented in this thesis was to collect dynamic measurements that would increase the knowledge of these dynamic properties.

## **1.4 Objectives and scope**

The overall objective of the work presented in this thesis is to chart the dynamic pressure development in a Francis turbine by measurements, and to gain a better understanding of the dynamic pressure phenomena which are most severe regarding runner fatigue. To approach this objective through the analysis of measured data, some challenges need to be addressed. Three targets were defined. The first of these targets was the development of measurement chains, enabling onboard pressure and strain measurements in both model and prototype Francis runners. Due to the rotating domain, rotating logging systems able to transmit or store measurement data is necessary. Also, sensors suitable for installation in the runner blade surface are needed. The second target was to perform measurements as elaborate as possible, to create proper data sets to be able to investigate the dynamic behavior of the runners. The third target was to investigate the measurement data in the time domain and in the frequency domain, and based on these investigations search for model-prototype and pressure-strain correlations.

The scope of the work is largely related to the preparation of the measurements. Integrating pressure sensors in the model runner blades and water proofing cabling for signal transmission are among the most challenging and time consuming tasks. Also, the preparation of a stand-alone logging system for the prototype measurements is elaborate.

It is a desire to compare the pressure measurements with results from Computational Fluid Dynamic (CFD) simulations. Such

simulations are performed by Andritz Hydro AG in Zürich, and the measurement data is used for further development and improvement of their simulating tools. A master thesis on transient simulations of the NTNU runner has started.

## **1.5 Previous work**

As hydropower technology has been utilized for more than a century, a lot of research has been performed by numerous scientific divisions. Among the first major works presented on dynamic instabilities was “Power swings in hydroelectric plants”, published in 1940 by W. J. Rheingans [5]. Since this, several authors have discussed the topic of dynamic problems in the draft tube of reaction turbines [6, 7], and proposed different solutions to mitigate the consequences [7-9]. Installing flow straightening fins in the draft tube has been proposed. This is not considered a viable solution due to adverse effects, such as cavitation. Air admission to reduce the impact of the instable draft tube flow is a common solution. This countermeasure is still being retrofitted into old units, and incorporated in the design of new units [10]. Research is now being carried out to investigate the effect of injected water. Axial injection through the runner hub [9] and tangential injection through the draft tube wall [11] are being tested at different research environments.

Large cooperative research projects have been carried out to push the development forward. Such projects are the FLINDT-project [12], followed by the HydroDyna project [13]. The goal of the FLINDT project was to create a database for validation and calibration issues of Computational Fluid Dynamics (CFD) of draft tube flow [14]. After FLINDT, the HydroDyna project was launched, with the objective to investigate the rotor stator interaction phenomenon and fluid structure coupling. The second phase of the project focuses on the rotor stator interaction and fluid structure coupling of reversible pump turbines with respect to high dynamic loads and influence on life span [13]. There is currently a focus on simulating rotor stator interaction using computer software. Keck and Sick [15] described the development of CFD over the last three decades, and the increase in possibilities this development has resulted in. For steady calculations, it is clear that

CFD is an invaluable tool when designing turbomachinery. The tools are now developed in such a way that also some dynamic problems can be predicted, such as the von Kármán vortex shedding and rotor stator interaction. However, larger scale dynamic problems are still too complex for numerical methods to solve accurately. In Ciocan et al [14], comparison of CFD and experimental results show very good agreement, and the CFD seems to capture transient phenomena and the draft tube flow field very well. However, the calculations performed were for single phase, and the model experiments were performed at high  $\sigma$  values to avoid the appearance of the cavitating vortex rope. Stein [16] (cited in [15]) described in his PhD thesis that accurate simulation of the draft tube vortex would require about  $\frac{1}{2}$  billion grid nodes (in addition to accurately described boundary conditions) in order to achieve the accuracy needed to predict the volume of vapor. The accuracy of this prediction is necessary to properly predict the frequency of the vortex, and the system dynamic response to this dynamic pressure. Today, simulations involving  $\frac{1}{2}$  billion nodes are too costly for design studies.

Numerical methods for system dynamics are readily available and continuously improved by researchers [17]. There are possibilities to include turbine dynamic behavior in the system dynamic software, however this is not yet in use commercially, and the accuracy of the results is not verified. As described in the previous paragraph, complete simulations of the draft tube vortex volume and frequency are not in use, so the resonance between system dynamics and turbine dynamics cannot be predicted. Another topic currently experiencing a great focus is the coupling between the dynamic flow field and the structural response, fluid structure interaction, such as in the HydroDyna project [14, 18].

As a summary on computer tools, CFD and FEM analysis are the main necessities when designing turbomachinery. As these tools now move toward an ability to capture transient phenomena, they need elaborate experiments for comparison and verification.

At the Laboratory for Hydraulics Machinery at Ecole Polytechnique Fédérale de Lausanne, EPFL-LMH, onboard model strain and pressure measurements have been performed in cooperation with both Alstom [19, 20] and Voith Siemens [21, 22]. Alstom has also

performed tests in their own laboratories [23]. Some tests used wireless transmission, while others used onboard signal conditioning and transmission via slip rings. These tests have all focused on low head units. The conclusion are that these tests give valuable knowledge about the dynamic behavior of the runner, but that the tests are too elaborate to use for all model test campaigns. Only tests involving runners designed for large head ranges were recommended for this kind of campaign.

Onboard measurements on prototypes have also been performed. Just after commissioning of the 447MW St. Marguerite 3 ( $\omega=0.44$ ,  $n_s=39.0$ ), large cracks were discovered in the runner blades. Coutu et al [1] performed a Root Cause Analysis, including onboard strain gauges in the prototype. Their investigation also included eigenfrequency tests in air and water, material evaluation, and static FEM calculations. Their strain gauges confirmed the calculated low static strains, but large dynamic strains were found. The only distinct frequency found in the strain was the guide vane frequency. After modifying the inlet, the guide vane frequency amplitude was clearly reduced. A rather odd countermeasure was also applied. It consisted of mounting 5 struts inside each hydraulic channel, physically connecting all runner blades to their neighboring blades. The struts were placed close to the blade trailing edge. Due to the stiffer structure, this countermeasure further reduced the guide vane frequency amplitude in the blade material. The effect on the hydraulic efficiency was not mentioned.

Bjørndal et al [24] performed onboard measurements on a medium head prototype Francis X-blade runner ( $\omega= 0.63$ ,  $n_s=56.5$ ). Comparison of FEM analysis and strain gauge measurements gave a good correlation for the mean stresses. Only four operating points were measured, not covering the area thought to have the largest dynamic stresses. They found that the maximum mechanical stress range exhibited the highest values at the lowest measured load (approximately 3% of rated output, described as speed-no load), and decreasing towards rated output. No frequency domain analysis was presented.

Bjørndal et al [25] also performed onboard strain gauge measurements at Frøystul power plant ( $\omega=1.02$ ,  $n_s=90.8$ ). The dynamic stress range was found to be largest at 45%, disappearing

into what seemed to be stochastic noise at 73% of BEP. No guide vane frequency was found in the runner blade trailing edge strain gauges. At 45% load one could find from the frequency spectrum that the dominant frequency was approximately 10 times the runner rotational frequency  $f_n$ . At other loads, this dominant fluctuation gradually changed frequency, up to about  $15 \cdot f_n$ . Due to this change, it was concluded that the fluctuation was caused by hydraulic forces, and not by mechanical natural frequencies in the turbine.

In the frequency plot from the strain measurements, the draft tube vortex frequency was clearly seen. At some part load operating points, the vortex rope frequency exhibited the largest amplitude, but at 45% load the vortex amplitude was about half of the  $10 \cdot f_n$  amplitude.

Lowys et al [26] performed extensive onboard measurement on two low head prototype runners. Due to several cracked runners, this field measurement campaign sought to explore the dynamic behavior of low head Francis prototypes. In their "Project 1" runner, they found a high level of dynamic stress in the entire part load region, with a maximum at about 70% of rated output, and significantly decreasing above this load. No frequency analysis was presented, so no information on the guide vane frequency was revealed.

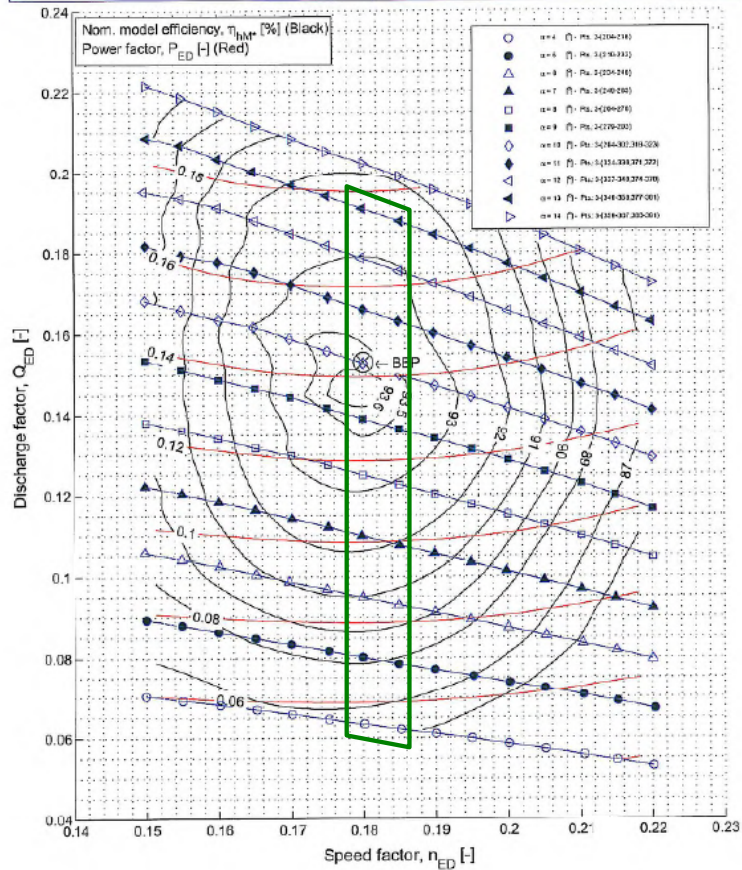
Lowys et al [23] compared pressure and strain measurements in low head model runners. They found that both dynamic strain and pressure were highly dependent on the test head, but that there were no distinct correlation between the areas of high dynamic pressures and high dynamic strains. A comment on model runner dynamic strain is presented later in this thesis, in Chapter 5.2.

The results from the St. Marguerite 3 investigation indicate that the vaneless space is of great importance. The results from the units with higher specific speeds tested by Bjørndal are different. For low head units, the meridional extent of the vaneless space is quite large compared to high head units. Also, if the runner blade leading edge is skewed (not vertical), a guide vane wake will enter differently at hub and ring, reducing the impulse on the blade.

If the guide vane frequency is of greater concern regarding runner lifetime, high head units should be more susceptible to fatigue. However, this does not seem to be a general rule, fatigue has occurred in both high and low head units. Hence one can probably not present a general rule that the guide vane frequency is the most severe cause for fatigue in all Francis runners, even if it is thought to be so for high head units.

## 2 Theoretical background

<b>NTNU</b> Waterpower Lab.		Project of: <b>Tokke</b>		Encl: <b>Encl. 16.138</b>	
		Document: <b>Mussel diagram (Model)</b>		Data file: Tokke-vkl080207-2_mod.txt	
Proj. no. - Test center: <b>340298.00 - 3</b>		Date/Sig.: <i>25-Feb-2007</i> <i>J.Rand</i>		Approval: <i>Ole G. Dahlbom</i>	
Model id: <b>VIG-1</b>	Manufacturer: <b>TOKKE-1</b>	Spiral case ID: <b>VKL-2006-1998</b>	Stay vane ID: <b>VKL-2006-1032</b>	Guide vane ID: <b>VKL-2006-1075</b>	Draft tube ID: <b>VKL-2006-1079</b>
$D_{st}(mm) = 349$ $H_{st}(m) = 20.30$ $\theta_{st}(^{\circ}C) = 19.4-20.8$ $\sigma_{st} = 0.16-0.2$ $n_{st}(-) =$ $D_p(mm) = 1779.9$ $Re_{p,1} = 4.053 \cdot 10^7$ $\Delta\eta_{v,s}(%) =$					



Tromsø, Test date: 08.02.2007, Operator: Jørgen Rørdal

Plot ID: P05\_Mod\_Hill\_Test\_3\_20070225.eps

Figure 2-1. Hill chart for the NTNU model runner [27]. Pressure pulsation model test range is marked by green, and was defined by plant head and flow range.



The Hill chart in Figure 2-1 show the operation of the NTNU designed reference runner. In the test rig, the turbine rotational speed and head is controlled. In the plant, the rotational speed is fixed and the head given by reservoir level; however the head loss varies with the operating point. This will result in a lower head at higher flows, hence increasing the speed factor slightly for high loads. To reduce this effect during the actual field test, another unit was operated with an opposite load pattern. This way the plant flow and head loss was kept approximately constant.

In Figure 2-1, the axes denoted by the speed factor  $n_{ED}$  and the flow factor  $q_{ED}$  are defined by:

$$n_{ED} = \frac{n \cdot D}{\sqrt{g \cdot H}} \quad \text{Eq. 1}$$

$$q_{ED} = \frac{Q}{D^2 \cdot \sqrt{g \cdot H}} \quad \text{Eq. 2}$$

where n = runner rotational speed  
 D = runner outlet diameter  
 g = gravitational constant  
 H = net head  
 Q = flow

In the Hill chart, the green area corresponds to the highest and lowest regulated levels of the upper reservoir, and this was used as the head range limits for the model tests.

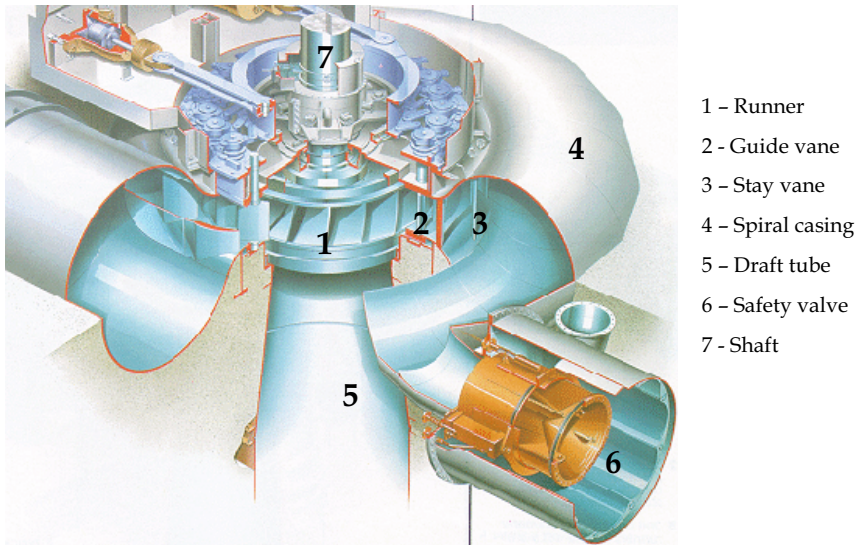


Figure 2-2. A view of the Francis turbine (ref. Kværner Brug AS)

## 2.1 Sources of pressure pulsations

When operating a Francis turbine at stable operating conditions, several hydraulic instabilities can occur. These are summarized below. Of the sources described, surge, rotor stator interaction and hydraulic instabilities were investigated. Cavitation bubble collapse, vortex shedding and system dynamic pressure fluctuations were not investigated, due to the chosen logging frequencies and periods. Rotating stall was not expected to be found, and not investigated.

### 2.1.1 Surge

Draft tube pressure pulsations in Francis turbines are well known phenomena. The first major work presented on this topic was performed by Rheingans in 1940 [5]. In the draft tube of a Francis turbine, the flow is determined by the flow exiting the runner. At best efficiency point (BEP), the flow direction is mostly parallel to the shaft axis. At operating points differing from BEP, a tangential velocity component is present. This tangential velocity component is the source of different phenomena. At loads below BEP, the direction of the tangential flow is in the same direction as for the runner rotation. At some loads, a cavitating rotating vortex rope can

be observed, with a helical shape. At loads above BEP, the tangential flow direction is in the opposite direction of the runner rotation. At higher loads, this results in a cavitated vortex core [6]. Helical vortices in swirling flows are phenomena present in several devices [28]. The rotating vortex rope is one occurrence of the helical vortex. The part load rotating vortex rope results in forces fluctuating radially in the draft tube. This might lead to vibrations in the system, and ultimately fatigue. At some power plants, the rotating vortex rope is so strong that it causes a pressure fluctuation that can propagate upstream through the runner, causing mass flow fluctuations in the waterway. These fluctuations will excite elastic pressure waves. If they coincide with resonance frequencies in the system they can cause large fluctuations. Common countermeasures include, among others, free or forced air admission [7]. The over load vortex core might cause mass flow fluctuations, that can propagate through the entire waterway causing power fluctuations from the unit.

Prior research has indicated that for a given draft tube shape, operating at Reynolds numbers  $Re$  found in turbines, the amplitude and frequency of draft tube surge pressure fluctuations depend only on the value of the draft tube swirl parameter,  $S$  [29]:

$$S = \frac{\Omega D_3}{\rho Q^2} \quad \text{Eq. 3}$$

where:

$\Omega$	=	flux of angular momentum
$D_3$	=	draft tube throat diameter
$\rho$	=	density
$Q$	=	discharge

The frequency of the rotating vortex rope differs from unit to unit. It often lies close to  $\frac{1}{3} \cdot f_n$  as observed by Rheingans [5], however it is reported to be in the range of  $\frac{1}{4}$  to  $\frac{1}{2}$  of  $f_n$ .

Examples of draft tube cavities for different loads can be seen in Appendix 9.4.

### 2.1.2 Rotor stator interaction

Rotor stator interactions are of general concern when dealing with turbo machinery. Rotor stator interaction can be categorized as two different phenomena: *Wake/rotor interaction* and *Potential rotor/stator interaction* [30]:

- Wake/rotor interaction can be assumed approximately steady in the stator reference frame, while they are unsteady in the rotor reference frame since the rotor is passing through wakes leaving the stator.
- The unsteadiness from potential rotor/stator interaction arises because both stator and rotor experience non-uniform pressure components.

The combination of these two effects results in a non-uniform velocity field entering the runner, as shown in Figure 2-3.

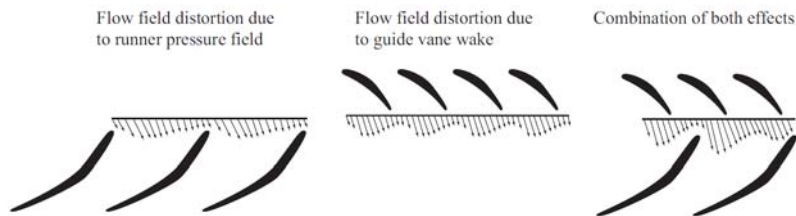


**Figure 2-3. Flow field at inlet of runner, from Nicolet et al [31], displaying runner and guide vane effects on flow velocity and angles.**

The different sources of vibration in turbomachinery are discussed in detail in Brennen [32].

The blade passing frequency is measured in the vaneless space in a Francis turbine. It is a form of the potential rotor/stator interaction, and is illustrated by Figure 2-4. It can be seen in the frequency spectra at a frequency equal to the number of runner blades multiplied by the runner revolution frequency,  $Z_r \cdot f_n$ . It can also be seen in turbines without guide vanes, resulting from the wake from the spiral casing tongue [33]. Blanco et al [34] performed a numerical and experimental study of pressure pulsations in a pump with four different runners of different diameter. Their spiral casing (diffuser) had no stay vanes, only the tongue. They

concluded that the level of pressure pulsations is highly dependent on the radial clearance between the spiral casing tongue and the impeller. The level of pressure pulsations and the unsteady force greatly increased as the impeller-tongue gap was reduced. It is likely that this is also true for Francis turbines, namely that the level of pressure pulsations will increase as the radial clearance between runner inlet and guide vane outlet decreases.

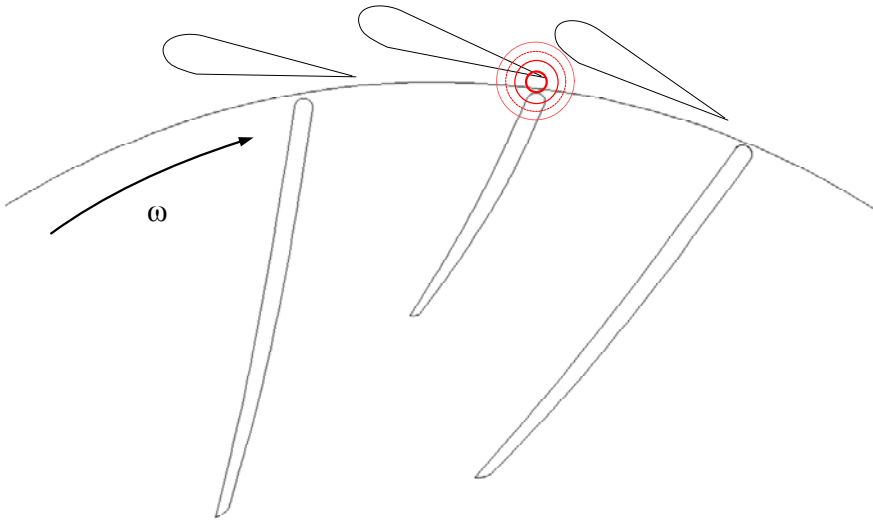


**Figure 2-4. Pressure pulse appearing when runner blade passes the guide vane**

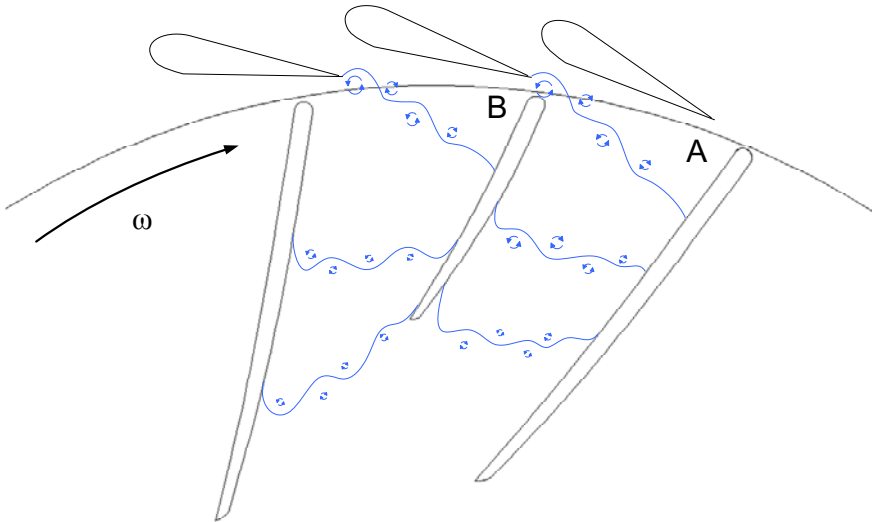


**Figure 2-5. Guide vane wake travelling through runner**

The guide vane frequency,  $Z_s \cdot f_n$ , is measured in the runner, and is in the wake/rotor interaction category. It is a result of the wake leaving the guide vane before it enters the runner, as shown in Figure 2-5. Jernsletten [35] tested a reversible pump turbine runner. It was first tested with its original runner design, and then the inlet diameter was reduced by 1.72% by cutting back the runner blade inlet. This reduced the amplitude of the guide vane frequency with a factor of  $\frac{1}{3}$ . To obtain the same effect in a Francis turbine without compromising on the runner blade design, the vaneless space should be increased in radial direction. However, increasing this gap in a Francis turbine results in a larger spiral casing, again increasing the construction costs. Due to the cost issue, the gap is kept very small.

The potential rotor/stator and wake/rotor interaction categorization could be used to argue that the blade passing frequency exists both in the rotating and stationary frame of reference, while the guide vane frequency does not exist in the stationary frame of reference. This is discussed in Chapter 5.2 Measurement results.

In addition to  $Z_r \cdot f_n$  and  $Z_s \cdot f_n$ , there will be a dynamic pressure fluctuation at  $Z_r \cdot Z_s \cdot f_n$ . This frequency can be measured in the vaneless space. Due to the high frequency (2975Hz at the Tokke replacement prototype), this frequency could not be detected in the measurements presented in this thesis.

In addition to  $Z_r \cdot f_n$ ,  $Z_s \cdot f_n$  and  $Z_r \cdot Z_s \cdot f_n$ , super harmonics can be found at  $m \cdot Z_r \cdot f_n$  and  $n \cdot Z_s \cdot f_n$ , where  $m$  and  $n$  are integers. Also, if a common factor exist between  $Z_r$  and  $Z_s$ ,  $Z_{cf}$  being an integer, it is possible to find sub harmonics at  $Z_r \cdot f_n / Z_{cf}$  or  $Z_s \cdot f_n / Z_{cf}$ . Due to the lower frequency, these frequencies will experience a lower dampening than the original excitation, and may consequently be of greater importance. Hence, when designing a turbomachine unit, one should try to avoid such a common factor [32].

### **2.1.3 Rotating stall**

Rotating stall is a well known phenomenon in turbomachinery in general, especially in compressors with large number of blades [32]. The phenomenon has not been reported in Francis turbines, however it has been observed in pumping mode of reversible pump turbines [33, 36]. The stall rotates in the same direction as the rotor, with a frequency of 0.5-0.7 times angular velocity of the runner. For rotating stall to occur, a high angle of incidence is necessary, in order to trigger flow separation.

### **2.1.4 Hydraulic instabilities**

Mechanical or hydraulic imbalance in the systems can result in hydraulic fluctuations, often seen at the rotational frequency  $f_n$ . One common source in Francis turbines is a hydraulic instability from the spiral casing. When designing the spiral casing, the area around the tongue will be a compromise between the ideal flow at the spiral casing inlet, the ideal flow through the last stay vane cascade of the spiral casing, and manufacturing issues. The result is sometimes a non-uniform pressure and velocity field in this region. Simulations of the Tokke spiral casing performed by Stückle [37] show that the Tokke spiral casing produced in late 1950's experience this non-uniform field. These fluctuations were found in the measurements performed during this thesis.

### **2.1.5 Cavitation**

Cavitation is seen as a high frequency and broad band disturbance in Francis turbines, so it is not considered a problematic topic with regards to fatigue, although cavitation bubble collapse can cause major erosive problems in hydraulic machinery in general [38]. Fluctuating pressure fields are proved to greatly affect the formation and collapse of cavitation bubbles [39]. Brennen [32] describes that cavitation indirectly can cause large pressure pulsation problems through the phenomenon “Partial cavitation oscillations”.

The draft tube vortex rope described in Chapter 2.1.1 is also caused by cavitation. However, the collapse of the bubbles from this cavity generally occurs some distance away from the draft tube wall, and hence does not cause cavitation erosion.

### **2.1.6 Vortex shedding**

When introducing structures into any fluid flow, the phenomenon of von Kármán vortex shedding appears [40]. This is known to cause fatigue failure of stay vanes in Kaplan turbines [41-43]. von Kármán vortices are also known to result in severe noise from Francis runner blade trailing edges, calling for modification of the trailing edge. The von Kármán vortices will also be one of the components of the guide vane wake. The von Kármán frequency at the guide vane trailing edge can be in the range of 1kHz and above (dependent on the flow velocity through the guide vane cascade) [42, 44].



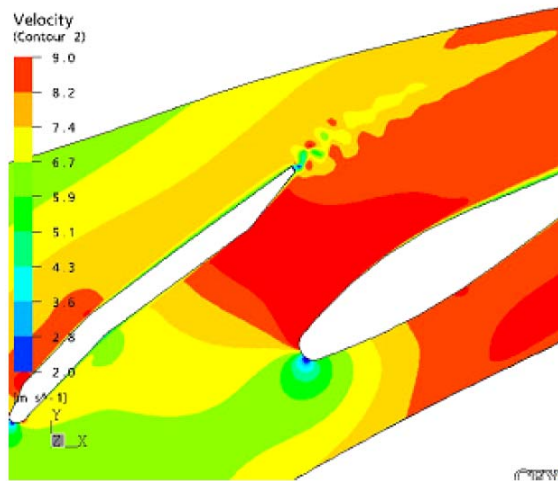


**Figure 2-6. Instantaneous velocity magnitude of a Kaplan stay vane, showing von Kármán vortex shedding [42]**

### **2.1.7 System dynamic pressure fluctuations**

So called U-tube fluctuations are common system dynamic features of large piping systems. They appear as large mass oscillations resulting from the flow acceleration or deceleration occurring when the load of the turbomachine is changed. The so-called water hammer is a system dynamic feature. This pressure pulse is the propagation of pressure information with the speed of sound, which can become violent if the closing time of the valve is shorter than the reflection time of the conduit. In addition, small changes in guide vane opening can excite elastic pressure pulses. If these coincide with turbine resonance frequencies, large amplitude pressure fluctuations can arise.

## **2.2 Measurement equipment background**

*Piezo (Greek): squeeze or press*

There are two main types of pressure transducers in use today, piezoresistive and piezoelectric. Piezoelectric sensors are based on quartz or silicon crystals. These pressure transducers tend to be very rugged, and have a very high natural frequency (resonance frequency), thus used to measure rapid processes. The main short-

coming is that they cannot measure static signals. When forces are applied to the sensing material in piezoelectric transducers, an electric potential is generated across the material. If the material is not short-circuited, the applied stress induces a voltage across the material.

Piezoresistive sensors can be either quartz based or strain gauge based. The main advantage of strain gauge based pressure transducers is that they can measure absolute static pressure levels. However, these have traditionally had lower maximum logging frequencies than piezoelectric sensors (although newer miniature semiconductor strain gauges feature high natural frequencies). These strain gauge based sensors consist of one or more strain gauges mounted on a diaphragm. When the diaphragm is subjected to pressure, it deflects, and the strain gauge changes the output. They are relatively slow, but can have a natural frequency that is more than high enough for quite a number of applications.

The output signal also affects the maximum logging frequency of the sensor. The output of e.g. a strain gauge is in millivolts. These signals are very fast, but vulnerable to noise generated by surrounding magnetic fields. One method to reduce this noise is to convert the signals from voltage (transducers) to current (transmitters). This conversion reduces the noise influence and allows for longer signal cables. But the voltage to current conversion drastically slows down the maximum logging frequency.

Due to the ability to measure static pressures, strain gauge based pressure transducers were used. In the draft tube wall pressure measurements, transmitters with current output were used, to reduce the influence of electrical noise. The bandwidths of the components used in the measurements are shown in Table 2-1 and Table 2-2. The logging equipment used in the model and prototype measurements is further described in Paper 1 and Paper 2.

**Table 2-1. Summary of data acquisition hardware used in model measurements**

Hardware	Type	Bandwidth	Range
SRI PMD 500e	Wireless transmitter / receiver for onboard sensors	2.1kHz (at chosen number of channels and bit resolution)	+/-45mVDC input signal
National Instruments NI-USB6212	Data acquisition card	250kSamples per second	4-20mA, 2-10V
Kulite XTE 190	Strain gauge based pressure transducer	~100kHz (300kHz natural frequency)	0-3.5 barA
Kulite LL080	Strain gauge based pressure transducer	~100kHz (300kHz natural frequency)	0-3.5 barA
Druck PTX 610	Strain gauge based pressure transmitter	1kHz	0-10 barA

**Table 2-2. Summary of data acquisition hardware used in prototype measurements**

Hardware	Type	Bandwidth	Range
National Instruments Compact RIO	Standalone controller	50kSamples per second per channel	Programmable
National Instruments NI-USB6212	Data acquisition card	250kSamples per second	4-20mA, 2-10V
Kulite XTE 190	Strain gauge based pressure transducer	~200kHz (700kHz natural frequency)	0-35 barA
Kulite LL080	Strain gauge based pressure transducer	~100kHz (380kHz natural frequency)	0-7 barA with overpressure protection
Druck PTX 610	Strain gauge based pressure transmitter	1kHz	0-10 barA

## 2.3 Analyzing techniques

### 2.3.1 Statistical tools

The results from the measurements are analyzed by means of statistical properties such as the mean (Eq. 4) and the standard deviation (Eq. 5). Standard deviation was used as the measure of spread in the fluctuations. Normal distribution was assumed, and  $\pm 2 \cdot \sigma$  used for 95.4% confidence interval, equivalent to the common peak-peak measure.

$$\bar{x} = \frac{1}{n} \sum_{k=0}^{n-1} x_k \quad \text{Eq. 4}$$

$$\sigma^2 = \frac{1}{n-1} \sum_{k=0}^{n-1} (x_k - \bar{x})^2 \quad \text{Eq. 5}$$

### 2.3.2 Spectral analysis

The most common tool to investigate time signals in the frequency domain is the so called fast Fourier transform, FFT. This is a mathematical algorithm to compute the discrete Fourier transform, DFT. The DFT is defined by [45]:

$$F(k\Delta f) = \sum_{n=0}^{N-1} f(n\Delta t) e^{-j(2\pi k\Delta f)(n\Delta t)} \quad k = 0, \dots, N-1 \quad \text{Eq. 6}$$

A DFT decomposes a time signal  $x=f(n \cdot \Delta t)$  into components of different frequencies. For a time series with  $N$  observations, the numbers of operations needed, and hence the time consumed, is a function of  $N^2$ . It is therefore a quite slow routine for longer data series. The FFT is an improvement of the DFT, and requires a number of operations proportional to  $N \cdot \log(N)$ . For large data series, this results in a significant reduction of computing time. The most common FFT algorithm is the Cooley-Tukey algorithm. This algorithm breaks up the original DFT into several smaller DFTs, in order to reduce the computational time. All DFT methods require a constant time step  $\Delta t$ .

In the prototype measurement, the logging chain featured some limitations. Due to internal buffer memory size, small “write-to-file pauses” appeared in the measurement result file. This is described in Paper 4. Due to these pauses, the time series from the measurements could be seen as an example of the “missing data point problem” arising in spectral analysis. When data points are missing, information on the physical process is lost. Also, because common spectral analysis methods require a constant time step  $\Delta t$ , the missing points will introduce an error in the time scale. Non-ideal solutions to this problem can for instance be truncation of the time signal where the data is missing. Truncation generally results in non-physical and spurious distortion when applied to time series before analyzing the time series with Fast Fourier Transform algorithms. This distortion is often seen as noise in the low frequency band. When the original frequency spectra is not known, these spurious results cannot be identified, hence the frequency spectra is not fully trustworthy.

Another non-ideal cure for this problem is to just add zeros for each missing time step, after removing the mean from the time series. This will not cause an error in the time scale, but will still introduce non-physical results.

A third non-ideal way to handle the missing data point problem is to extrapolate the measured data into the time window where data is missing. There are several different tools to extrapolate time series. For time series containing only sine shaped fluctuations, extrapolation can be an appropriate countermeasure. However, when dealing with time series composite of the several non-sine signals, this method introduces errors and noise.

As the measured time series from the prototype measurements consist of several smaller blocks with a constant time step, an option would be to perform a FFT on each block, and average the results. However, because each block is short, the frequency resolution would be far from satisfactory. This method also introduced a significant level of white noise.

In geophysics, the missing data point problem is a well known problem, from when satellites transmitting measured signals are in the shadow of the earth. The normal countermeasure is known as

the Lomb normalized periodogram [46], also known as the Least-squares spectral analysis. The reason why this method works better for the missing data problem is that it weighs the data on a “per-point” basis, instead of on a “per-time interval” basis. This is contrary to FFTs. The Lomb method is computationally much more expensive than regular FFT methods, however it allows for non-uniform time steps in the time series. The major practical difference from a regular FFT is that instead of a single time step  $\Delta t$ , the entire time array from the measurements is inserted in the method as the second input, in addition to the array of measured values. In this way, a frequency spectrum can be obtained, without introducing errors from truncation, zero insertion or extrapolation. Despite the significant increase in computational time, the Lomb normalized periodogram was used in the analysis of the prototype values presented in this thesis. One aspect that one has to be aware of using the Lomb normalized periodogram is that the results does not respect the Nyquist frequency,  $f_N=f_s/2$ . Hence, it seems like one can read frequencies higher than the Nyquist frequency from the results. These results are not to be trusted. Due to this, the time series was passed through a low pass filter with a cut-off frequency of half the logging frequency  $f_s$  before inserted into the Lomb procedure.

The Lomb normalized periodogram is defined as:

$$p_N(\omega) = \frac{1}{2\sigma^2} \left( \frac{\left[ \sum_{k=0}^{n-1} (x_k - \bar{x}) \cos \omega(t_k - \tau) \right]^2}{\sum_{k=0}^{n-1} \cos^2 \omega(t_k - \tau)} + \frac{\left[ \sum_{k=0}^{n-1} (x_k - \bar{x}) \sin \omega(t_k - \tau) \right]^2}{\sum_{k=0}^{n-1} \sin^2 \omega(t_k - \tau)} \right) \quad \text{Eq. 7}$$

where

$$\tau = \frac{1}{2\omega} \arctan \left( \frac{\sum_{k=0}^{n-1} \sin 2\omega t_k}{\sum_{k=0}^{n-1} \cos 2\omega t_k} \right) \quad \text{Eq. 8}$$

As long as one has a constant time step (or use methods such as the Lomb method) one can be quite certain of the frequency from any spectral analysis technique, as long as the time series input is long enough to ensure a sufficient frequency resolution. However, the

resulting amplitude from any spectral analysis always entails a certain numerical uncertainty. Therefore, the spectral analysis should not be used alone to investigate time signals. When finding dominant frequencies from the spectral analysis, the amplitudes should be checked in the time series, and by filtering the time signal.

When interpreting results from FFT frequency analysis tools, it is important to be aware of harmonics in the signal. When a signal is periodic but not sinusoidal, higher harmonics may be excited [32]. These harmonics are physical fluctuations in the system, with a frequency as an integer multiple of the original frequency.

One should also be aware of aliases, which are false frequencies appearing from the frequency analysis. In a measured signal, there will always be frequencies above the folding (Nyquist) frequency  $f_N$ . These frequencies will be projected according to a folding diagram [45]. This is illustrated in Figure 2-7. Here, a frequency at  $1.6 \cdot f_N$  (or  $2.4 \cdot f_N$  and  $3.6 \cdot f_N$ ) will be shown as a frequency at  $0.4 \cdot f_N$ . A common countermeasure to remove unwanted frequencies from a measured signal, is to use filter functions. However, electronic filter functions exert the same result as the FFT. If the measured signal includes a fluctuation close to  $f_s$  or close to an integer multiple of  $f_s$ , the filter does not remove these frequencies. This is due to the fact that the true physics of these fluctuations are not captured in the measurement, because the logging frequency is not high enough. Hence, one should have knowledge of all frequencies in the system, and choose a logging frequency sufficiently high to capture all physical fluctuations in the system. This is often difficult, due to the fact that there are often high frequency sources in a system, such as cavitation and von Kármán vortices.

As mentioned, the logging frequency selected for the prototype measurement was  $f_s=1,613\text{kHz}$ . The highest rotor stator interaction frequency in the Tokke turbine is  $175\text{Hz}$ , and is well below the folding (Nyquist) frequency. When measuring non-sine signal, a higher number of points per cycle would be preferable to obtain a proper amplitude prediction. However, due to hardware limitations described in Paper 2, the logging frequency was not increased.

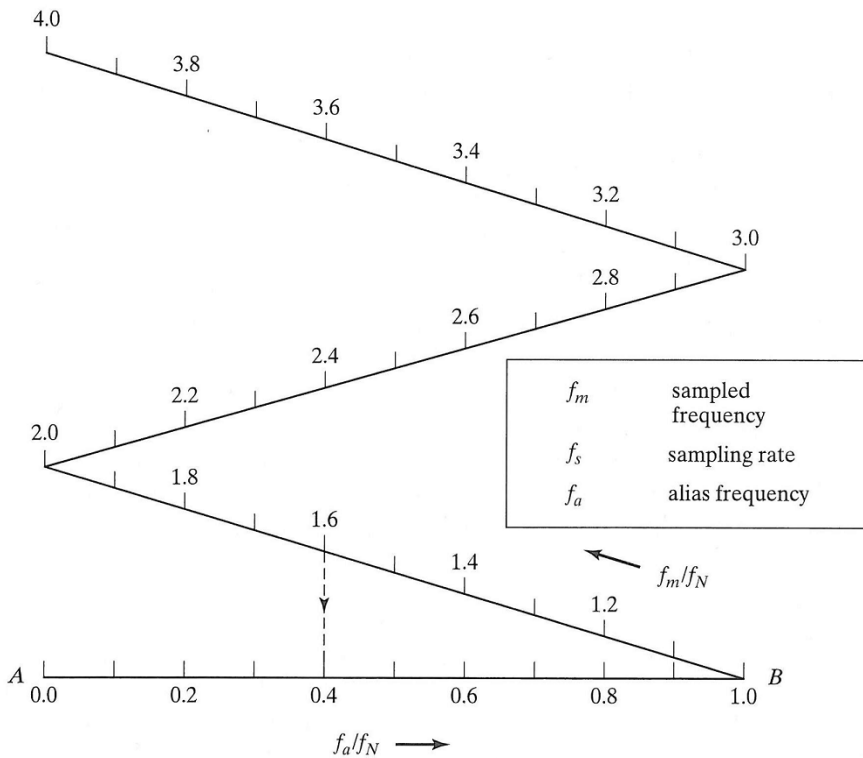


**Figure 2-7. Folding diagram [45].**

When investigating time series from more than one sensor in the same system, cross correlation can be a useful tool. The phase between the signals can be determined, and together with knowledge of the placement of the sensors one can determine whether the pressure is fluctuating in a rotating or axial manner.

When cross correlating simultaneously sampled signals, the phase of each frequency can be found. Hence, one must know the frequency to investigate. This can be done by regular frequency analysis. If the phase is zero between two signals measured at different tangential positions, this implies that the pressure pulsation is a so called pure pulsation, i.e. in the axial direction. If there is a phase shift between the signals, this indicates a rotating nature of the pressure. Cross correlation can also be used for the onboard sensors, to look for properties rotating inside the runner.



The cross correlation used in this work was computed in LabView. The algorithm used was called Cross Spectrum, which uses a FFT to determine the cross amplitude and phase.

The cross power  $S_{xy}$  can be defined by:

$$\begin{aligned} X(f) &= F\{x(t)\} \\ Y(f) &= F\{y(t)\} \\ S_{xy} &= X^*(f) \cdot Y(f) \end{aligned} \qquad \text{Eq. 9}$$

where  $X^*(f)$  is the complex conjugate of  $X(f)$ .

## **3 Measurements**

In this chapter, a brief overview of the model and prototype runner measurements is presented. They are described in detail in Paper 1 and Paper 2.

### **3.1 Model measurements**

The model measurements were performed in the Waterpower Laboratory at NTNU. A lay-out of the test rig from pressure tank to draft tube tank is shown in Appendix 9.3. Two model runners were designed during the Tokke project. One is designed by Andritz Hydro AG. This is the homologous model of the replacement runner for Tokke power plant, and was used for the development, verification and Model Acceptance Test. This runner has 17 runner blades. The second runner is designed by NTNU as a splitter blade runner with 15+15 blades, to serve as a reference runner for the test stand. By measuring the reference runner before and after the Andritz model runner, the stability of the test rig could be verified.

After these tests were finished, both runners were made accessible for onboard instrumentation, as described in Paper 1 [47]. Spare runner blades were manufactured for both runners, and pressure transducers integrated into these blades. The signal cables were transferred through the crown of the runner and through the shaft. Water proofing was applied to prevent water from following the cable passage.

As described in Paper 1, miniature strain gauge based pressure transducers were chosen for the onboard pressure measurements. When integrating the sensors into the runner blades, the blade material thickness of only 2mm at the outlet was decisive. Also, it was necessary to be able to measure the absolute pressure development, so piezoelectric sensors were not an option. The sensors chosen were small enough for blade integration, and featured a natural frequency of more than 1000 times higher than the maximum expected measured frequency.

Two different wireless systems were tested before a system for the measurements were chosen. These were the Microstrain V-Link and the Summation Research PMD 500e. Connecting 4 full bridge sensors and using a logging frequency of 2kHz, the Microstrain V-link would supply only 8bit resolution, while the PMD 500e supplied 16bit. Both units are miniature transmitters with 70 meters line of sight transmission range and high G capabilities. Due to the difference in resolution, the PMD 500e was the obvious choice. This system feature onboard programmable gain and signal filtering (anti-aliasing protection), AD-converter and multiplexer board. The receiver feature transmission error correction, DA-converter, temperature compensation for transmitter, and output signal conditioning. Power is supplied by a 9V battery package, so no slip rings are necessary.

## **3.2 Prototype Measurements**

### **3.2.1 Description of the plant**

Tokke power plant was commissioned in 1961, as the largest plant in Norway at the time. It has four units of 110MW each, operating under a nominal head of 377 meters. It is one of several plants in a larger system. It utilizes the head between Vinjevatn and Bandak, both located in Telemark, Southern Norway, see Figure 3-1. The upper reservoir also serves as the lower reservoir for Vinje power plant, so the head available is strongly influenced by this neighboring plant. By operating the two plants together, the Vinjevatn level is quite stable. The lower reservoir for Tokke, Bandak, is strictly regulated due to tourism. Hence, the allowable variation in water level is only 0.2 meters. This results in a very stable  $\sigma_{\text{plant}}$ .

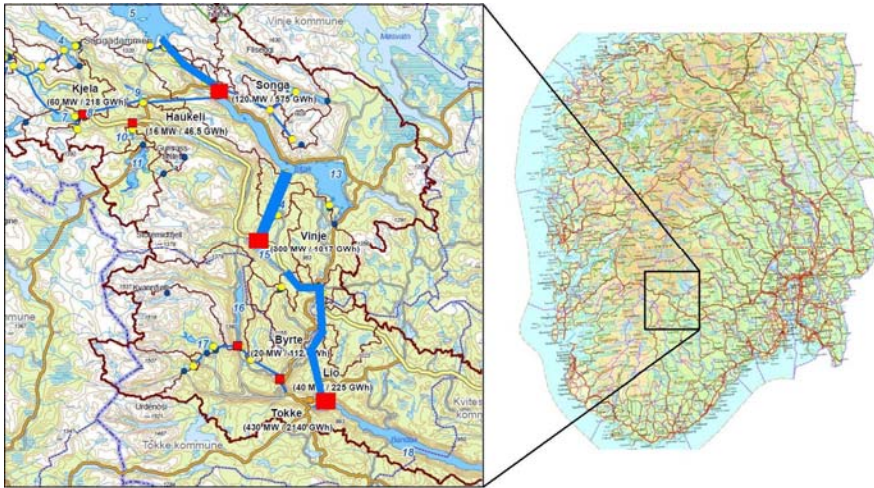


**Figure 3-1. Parts of the Tokke regulation area. The large red markers show Songa, Vinje and Tokke power plants, and the blue lines indicate the tunnels feeding the plants.**

Due to long and narrow head race tunnels, the head loss while operating all four units is significant (up to 16 meters). It is so large that it is not possible to simultaneously produce more than 100MW in each unit. Improvement of the tunnels was discussed, but found too costly. Since commissioning, the units have operated with only minor upgrades.

By the time this thesis is published, complete refurbishment of two units is finished, and refurbishment of a third unit has started. All major mechanical parts are dismantled and overhauled. The runners are replaced. The original runner was manufactured by Kværner Brug AS, and was of splitter blade design with 15+15 runner blades. It has operated well throughout its lifetime. There have been no reports of cracks or cavitation, but the runners are known to be very noisy. Sound levels of 120dB have been reported. The replacement runners now installed in two units have improved efficiency, and operate with a significantly reduced level of noise.

For the measurements on the replacement runner, the sensors and logger used are described in Paper 2. The same onboard pressure transducers were used as for the model measurements, in the same

relative position on the blades. However, no permanent alteration of the blade surface was allowed, so the sensors were fixed directly to the blade surface. Also, the same vaneless space transducers were used in the same relative position as for the model tests.

## **4 Summary of papers**

In this chapter, a brief summary and discussion of all papers are presented. The full length papers are found in Part 2 of this thesis.

### **4.1 Paper 1**

#### **Onboard Pressure Measurements in Francis Model Runner Blades**

*Kobro, E., Dahlhaug, O. G., and Nielsen, T., 2008, "Onboard Pressure Measurements in Francis Model Runner Blades", Proceedings from the 24th IAHR Symposium on Hydraulic Machinery and Systems, Foz Do Iguazzu, Brazil, ISBN 978-85-60858-13-1.*

The paper describes the preparation of a logging chain suited to perform onboard pressure measurements in the two model runners available in the project. A procedure for the installation of pressure transducers integrated into the runner blades is described.

The experience gained during the installation indicates that this method can be used for several applications. When dealing with sensors in fluids such as water, the major concern is water proofing. To resist corrosive fluids, sensors are often delivered with a cable jacket consisting of PTFE (polytetrafluoroethylene), commonly known by the brand name Teflon. This should be avoided, due to the fact that it is very complicated to bond epoxy to PTFE. Hence, the risk of water intrusion increases greatly with the use of PTFE. This is thought to be the reason that several onboard pressure transducers failed during the tests.

As described earlier in this thesis, an SRI PMD 500e telemetry system was used, with multiplexer, temperature compensation,

transmission of digitalized signals, and amplification in the receiver.

The cost of preparing such a system is considerable, both for equipment purchase and time for installation. Hence, it is most useful for special laboratory measurements, and is not suitable for standard model test campaigns.

After the paper was published, the procedure presented was used to install LL080 pressure transducers and strain gauges in a pump runner at NTNU. The procedure is also currently being used for installing the same onboard pressure transducers in the impeller of a wet-gas compressor at NTNU, with the same telemetry system.

## 4.2 Paper 2

### **Onboard Pressure Measurement in High Head Francis Prototype Runners**

*Kobro, E., Gamboa, A., Bloch, R., and Nielsen, T. K., 2009, "Onboard Pressure Measurement in High Head Francis Prototype Runners", Proceedings from the 3rd IAHR International Meeting of the Workgroup on Cavitation and Dynamic Problems in Hydraulic Machinery and Systems, Brno, Czech Republic, ISBN 978-80-214-3947-4.*

The paper presents the logging chain used for the two field tests performed at the Tokke power plant. Again, the importance of proper water proofing was illustrated. In the first test performed on the original Kværner runner, 6 pressure transducers were installed in the runner blade surface. The programmable logger was installed in the runner centre. The cables were secured with different epoxies. However, water managed to enter the cable insulation, passing inside the shield through the water proof connector. Hence, water entered the connectors of the controller, which malfunctioned. There was only a minor amount of water in the controller compartment, but the logger was permanently destroyed.

The next field test was performed on the replacement runner delivered by Andritz Hydro AG. Here, the same pressure transducers were installed in the same relative positions as for the Kværner runner and for the model runners. In addition, several strain gauges were installed. A different purpose built waterproof lead-through was used, to avoid the water intrusion experienced in the Kværner runner. The cables were covered in a way that would minimize the hydraulic disturbances.

The logger featured pre-programmable standalone capabilities. Hence, it could read the sensor channels following a predefined operating pattern. This pattern covered full range load ramps and stable operating points over the range.



Three piezoelectric pressure transducers were installed in the runner inlet pressure side. This had to be done while the runner was in the workshop, due to the poor accessibility to the runner inlet while the runner is installed in the turbine. Due to the harsh operating conditions during commissioning tests, cables to the runner inlet transducers were damaged, so no data was obtained from the inlet. One of the runner outlet transducers malfunctioned at turbine start up. The remaining 5 outlet transducers and all 16 strain gauges functioned well during the measurement. The logging unit proved to function well. Together with sensors in the stationary domain, this setup provided extensive measurements data.

The water proofing experience from the model tests arose again. The main conclusion concerning the installation of the equipment is that great care must be taken when choosing means for fixing the equipment to the wetted surfaces. Bonding of adhesive to cables and structure is imperative.

### 4.3 Paper 3

#### **Data Analysis from Onboard Francis Model Runner Pressure Measurements**

*Kobro, E., Nielsen, T. K., and Dahlhaug, O. G., 2010, "Data Analysis from Onboard Francis Model Runner Pressure Measurements", The 13th International Symposium on Transport Phenomena and Dynamics of Rotating Machinery, Honolulu, Hawaii, USA.*

In this article the analysis of the measurement data from the NTNU model runner is presented. Data was post processed using statistical methods and FFT analysis. The known dynamic pressures appearing in Francis turbines were isolated. Then the amplitude for each sensor and operating point was extracted. It was evident that the largest amplitudes found in the rotating system were at the guide vane frequency. It was also discovered that the draft tube surge was propagating both downstream and upstream the runner. If this surge is in phase with some system dynamic frequency in the plant, they can cause significant stability issues. Due to the non-homologous conduits of the model test stand, the effect in the prototype runner cannot be commented based on model tests.

Due to the high frequency and high amplitudes of the guide vane frequency, this dynamic pressure source would be the most crucial with respect to runner life time.

An interesting observation in the guide vane frequency amplitude development was a significant dampening between the third and fourth section of transducers. As illustrated in the paper, the possible explanation is that the guide vane wake develops differently through two neighboring splitter blade channels, and that the result of this difference is that the wakes meet in slight counter phase after the splitter blade outlet. Another explanation is that the sensors are placed differently with respect to stream line length when comparing pressure and suction side (see Chapter 5.2 in this superstructure). These statements will have to be verified by transient CFD.



## 4.4 Paper 4

### **Analysis of Onboard Pressure and Strain Measurement Data from High Head Francis Prototype Runner, and Discussion on Runner Lifetime**

*Kobro, E., and Nielsen, T. K., 2010, "Analysis of Onboard Pressure and Strain Measurement Data from High Head Francis Prototype Runner, and Discussion on Runner Lifetime", Journal of Fluids Engineering (paper under review, submitted on February 24<sup>th</sup>, 2010)*

This paper presents the analysis of the measurements performed on the Andritz replacement runner. Due to logging chain limitations, difficulties in the frequency analysis appeared. This was solved by replacing common frequency analysis tools with methods used in geophysics. The method is called Lomb normalized periodogram, as describes in Chapter 2.3 of this thesis.

The result from the analysis is that the only significant strain amplitude in the runner is caused by the guide vane frequency. This fits very well with onboard strain gauge measurements performed on another high head Francis unit [1], but differs from what was obtained from low head Francis strain measurements [23, 25]. The reason for this can be explained by increased radial distance of the vaneless space [48]. Low head units often have more skewed inlet edges than high head units, resulting in the guide vane wake entering the runner channels non-uniformly.

The operating points that exhibit the largest strains are clearly identified. On the pressure side, the pressure transducers show the same tendency as the strain gauges. The pressure on the suction side has a different development. This is believed to be the result of the very low pressure occurring close to the runner outlet cone. The suction side sensors can "see" the draft tube cavity, where the pressure is at the vapor pressure of water.

The topic of fatigue is also briefly discussed in the light of the measured data.

When investigating these results in the light of Antonsen [48], a conclusion is that when new high head units are built, the vaneless space should be made larger. This will increase the dimensions of the entire unit, and is hence a very costly countermeasure. However, it will reduce the risk of runner fatigue failure.

## **5 General discussion**

### **5.1 Data acquisition hardware**

When measuring properties in a rotating system, more limitations occur than for measurements in stationary components. The rotating data logger requires either onboard storage or some sort of transmission. Transmission can be utilized either via slip rings or radio signals. If analog signals with high frequency components are sent directly via slip rings, noise induced in the slip ring might cause problems. One solution can be to digitize the signals before the slip ring and use error correction software at the receiving end of the slip ring. Another solution can be to avoid slip rings by using radio transmission. For model tests, there is generally not enough physical space for systems with onboard storage. For this reason, and because there was a desire to investigate high frequency components, a telemetry system was chosen. For the prototype measurement, there was sufficient space to install a controller with onboard storage inside the runner cone.

As with the development of all new logging chains, challenges did arise, and they were solved. The logging chains chosen had some limitations. For the model measurements, the telemetry system was not capable of reading more than 4 channels. In the NTNU model there were 25 onboard pressure transducers and in the Andritz model there were 18 transducers. Hence, simultaneous logging of all rotating sensors was not possible. To be able to correlate sensors from different logging series, a key phaser (position indicator) was mounted on the shaft to determine the tangential position of the instrumented runner channel.

For the prototype measurement, the channel number was not a limitation. The system could be set up with the number of channels needed. However, the internal buffer memory of the controller was

quite limited, so only shorter periods of simultaneous logging were possible. This resulted in a challenge for the common frequency analysis tool. This challenge was overcome by using a computationally more expensive frequency analysis tool, as described in Chapter 2.3.2. This tool produces the same output as regular FFT algorithms, even with uneven input time scale. In addition to the rotating measurement equipment, dynamic pressure was measured in the draft tube and in the vaneless space. To correlate the stationary and rotating measurement chains, a key phaser on the shaft was used.

Onboard electronics in turbomachinery experience strict limitations concerning physical size, and must be able to resist G-forces. The telemetry transmitter in the model experienced about 20 G continuously, while the onboard logger in the prototype experienced about 9 G. The telemetry system was designed to withstand 5000 G continuously, but the onboard logger in the prototype was only guaranteed for 5 G continuously (up to 50 G half sine shock). The manufacturer nevertheless believed the system would be able to withstand 9 G continuously, and it was decided to rely on this.

## **5.2 Measurement results**

The geometrical scale between the Tokke prototype and model runners is 5.1:1, and the ratio between prototype and model output is in the order of 1000:1. Hence, the loading of the model runner is much lower. Also, due to the smaller physical size, the model is a structure with greater stiffness than the geometrically homologous prototype. Hence, it was not expected that strain measurements in the model runners would produce any results. Still, Andritz wanted to perform such measurements, in order to verify their numerical tools. The results of these tests confirmed the hypothesis; no strains were measured in the Andritz model runner.

Measurements of strain in the Andritz prototype showed that the guide vane frequency is the significant frequency in the blade strain. This corresponds very well with the findings of Coutu et al [1]. The Tokke prototype measurement featured strain gauges in the direction parallel to the flow and perpendicular to the flow. When investigating the perpendicular and parallel strains in the

same position of the blade, it was evident that these strains were fluctuating in counter phase. For a 2-D stress case, the Poisson ratio should be  $\sim 0.3$ , describing the transverse compression when a material specimen is subjected to axial tension. The ratio between the measured tangential and perpendicular strains was found to be approximately 0.2. The deviation from the 2-D Poisson ratio may be explained by the possibility of a 3-D strain situation in the blade, and due to the assumption of main strain direction perpendicular to the stream line.

Norconsult AS, by Halvard Bjørndal, performed onboard strain measurements in turbines very similar to the Tokke turbines. In the confidential report, he states that stress amplitudes at the guide vane frequency is dominating the stress variations at all load conditions. This corresponds very well to the findings from the Tokke runner.

Siwani [49] presents parts of a strain gauge measurement performed by Norconsult at Tonstad power plant ( $\Omega=0.27$ ,  $n_s=24.4$ ). A strain gauge rosette was installed. The results from the rosette is presented, and used to calculate the main strain direction. The calculated direction was close to, but not exactly, perpendicular to the stream line, as assumed in the previous paragraph.

In the pressure transducers in the rotating domain, the dominant frequency was the guide vane frequency in all runners. The draft tube vortex rope frequency was clearly evident in the runner channel of the NTNU model runner, however with lower amplitudes than the guide vane frequency in general.

Sick et al [41] states that the main source of vibration in reversible pump turbines is rotor stator interaction. In Francis turbines, phase resonance of rotor stator interactions might lead to unacceptable vibration amplitudes, as discussed by Dörfler [50].

Although vibrations in the turbine structure and strain fluctuations in the runner blades are not necessarily dependent on each other, both can be caused by rotor stator interaction. So the findings from both the prototype and the model measurements performed on the Tokke runners, and the strain measurements at St. Marguerite [1], are in accordance with Sick et al and Dörfler.



In chapter 2.1.2 it was proposed that the blade passing frequency exists both in stationary and rotating components, while the guide vane frequency only exists in the rotating components (i.e. the runner). The results from the model measurements presented in Paper 3 only partly agree with this statement. The guide vane frequency is not seen in the vaneless space; however the blade passing can be seen in the draft tube cone. This indicates that the blade passing pulsation has traveled from the vaneless space and through the runner. However, in the prototype measurements, the blade passing frequency is not found in the draft tube, nor in the runner. Hence, it is likely that the blade passing frequency measured in the model draft tube is due to vibration of the test stand, and not pressure propagation through the water.

One observation from the NTNU model runner measurement was that the dampening of the guide vane wake amplitude was different in the pressure and suction side of the hydraulic channel. See Figures 5 and 6 in Paper 3 – Data Analysis from Onboard Francis Model Runner Pressure Measurements. In Figure 5-1 and Figure 5-2, the normal operating points are plotted. It can clearly be seen that for sensor number 3 on the pressure side, the amplitude is higher than for sensor number 3 on the suction side.

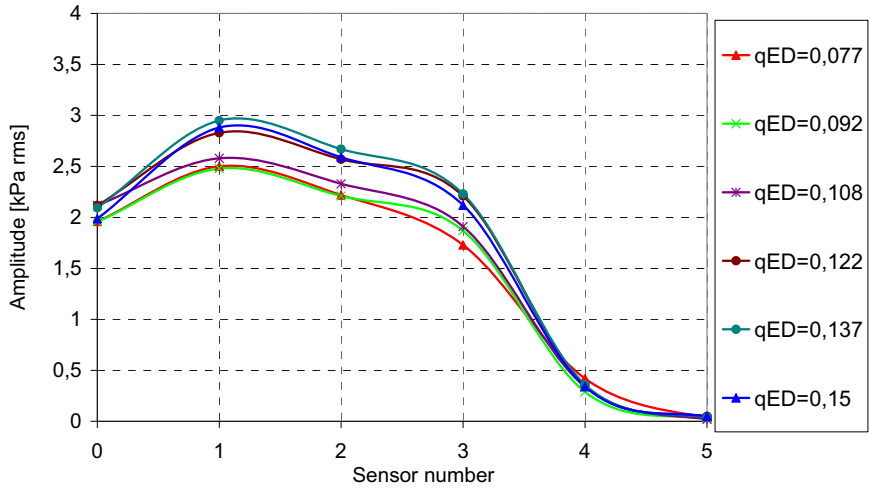


**Figure 5-1. RSI frequency amplitude, pressure side. Sensor 0 is in the vaneless space, sensor 1-4 is in the runner (see Figure 5-3), and sensor 5 is in the draft tube cone.**

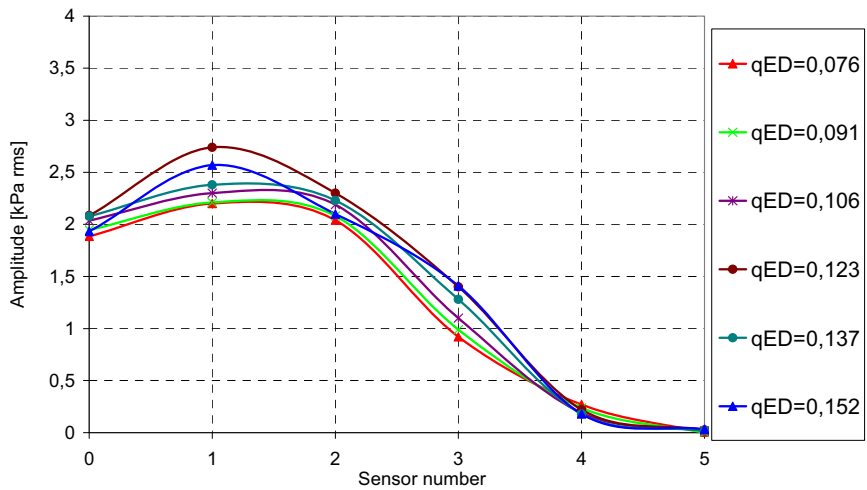


**Figure 5-2. RSI frequency amplitude, suction side. Sensor 0 is in the vaneless space, sensor 1-4 is in the runner (see Figure 5-3), and sensor 5 is in the draft tube cone.**

The sensors were placed at the same radius on pressure and suction side of the blade. This means that the pressure and suction

side sensors at e.g. radius 3 are placed differently compared to a line perpendicular to the flow direction, see Figure 5-3.

It is assumed that there is some interaction between the two flows exiting the splitter blade channels. The guide vane wake enters the two channels at different points in time, and the velocity is somewhat higher in the channel A than in channel B. The cause of the higher velocity in channel A is that the splitter blade outlet, Point P in Figure 5-3, is shifted somewhat towards channel A, compared with the mid line between the two channels. This is a design feature of the splitter blade runner, to obtain a smoother velocity profile across the channel downstream the splitter blade outlet. The result of these two facts is probably that the wakes meet slightly out of phase, and the wake amplitude is reduced. This process will probably smooth the velocity field at the outlet. The process appears at the splitter blade outlet, which is some distance away from the two sensors at radius 3.

One assumption made in the papers is that information of the mixing process at the splitter blade outlet does not reach the full blade surface on the pressure side until the flow has passed the radius 3. The dashed line in Figure 5-3 is perpendicular to the main flow in each channel, and reaches the blade surface differently on the pressure and suction side. Hence, the information from the mixing process does not reach the pressure side blade surface radius 3. This can explain the difference between Figure 5-1 and Figure 5-2, which indicate different dampening on the suction and pressure side.

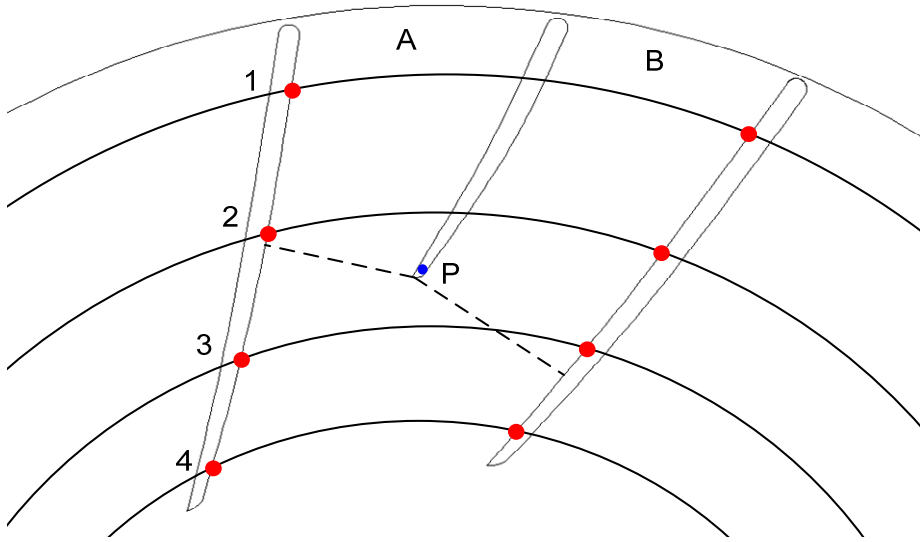


**Figure 5-3. Runner channel (A and B) with sensor radii (1-4)**



## 6 Conclusion

The objective of the work presented in this thesis was to chart the dynamic pressure development in Francis runners, and to gain a better understanding of the dynamic pressure phenomena from analysis of measurement data. To approach this objective, three targets were defined. The first target was to develop measurement chains for model and prototype onboard measurements. The second target was to perform tests as elaborate as possible. The third target was to investigate the measured results in the time and frequency domain, and based on these investigations search for model-prototype and pressure-strain correlations.

The two first targets were met successfully. Due to time limitations, the third target was only partially met. The investigation of a model-prototype pressure correlation and a prototype pressure-strain correlation is started, but the remainder of this investigation is left for further work.

It was expected that the development of the logging equipment would cause difficulties. Water proofing of electronics has been reported to be challenging. Also, transmission of data from the rotating runner required special attention.

Most of the equipment functioned well during the tests. The data transmission systems met the required specifications, although with some restrictions. In the model it was possible to measure only a limited number of channels, so all channels could not be recorded simultaneously. The signals could be monitored continuously during the tests. Due to the onboard storage in the prototype setup, it was not possible to inspect the stored time series until the test was completed. However, all channels could be recorded simultaneously. Due to hardware limitations, more computationally expensive methods than commonly used were necessary in the post processing work.

The dominant pressure fluctuation found in the model runner was the guide vane frequency. It was expected that this would be a pronounced fluctuation. Apart from at the blade outlet at part load, this frequency was the only dominant frequency for all load points. This was not expected. The draft tube vortex was thought to have a larger influence. In the NTNU model runner measurements, it was discovered that the guide vane frequency was significantly dampened towards the outlet, and more dampened on the suction side than on the pressure side. In the prototype strain and pressure measurements, the guide vane frequency was the only significant frequency. In the strain, it was observed a Poisson-ratio at about 0.2 when comparing strain perpendicular and parallel to the flow direction. The deviation from the ideal Poisson ratio of 0.3 is believed to be influenced by the assumption of main strain direction perpendicular to the flow.

Comparing the results from the high head turbine with previously published measurement results on low head Francis units, it seems that the guide vane frequency appear different in the strain measurements. This can be explained by the difference in radial distance from guide vane outlet to runner blade inlet in high and low head units, and that the inlet edge of low head units are more skewed than in high head units.

In the model runner, the Rheingans frequency was discovered to propagate upstream the runner, almost undampened. Due to the relatively low number of cycles caused by the draft tube vortex rope and moderate strain amplitudes measured, this frequency does not pose a threat regarding fatigue. Still, if in resonance with other system frequencies, it can cause large system fluctuations and power swings.

With respect to runner fatigue in high head Francis turbines, amplitude and number of cycles are the important fluid dynamic variables. Hence, data collected during these studies indicate that mitigation of the guide vane frequency should be of greatest concern.

## **7 Further Work**

Hydropower is often referred to as a mature technology. Does such a thing as a “mature technology” really exist? Especially given energy challenges facing the world at the beginning of the 21<sup>st</sup> century, hydropower is likely to play a significant role in the future energy matrix. Hence, researchers must pursue the improvement of existing technology, and exploit existing technology in new applications. Changing operating regimes, due to the regulating capacities demanded by new renewables, will probably be one of the larger challenges the hydropower community will face.

### **7.1 Pressure scale up, and pressure-strain correlation**

As CFD still has some way to go to be able to accurately predict dynamic phenomena in complex flows, measurements of model and prototype turbines will still be important. For hydraulic efficiency measurements, there exists an empirical scale up relation from model to prototype efficiency values [51]. Some research groups have started to investigate the relation between model and prototype values for dynamic pressure. Jacob et al [52] and Fisher et al [53] investigated draft tube pressure in model and prototype turbines, and they found clear correlations. Jacob et al states that “General features of the part load precession and the full load pulsation were the same on model and prototype”. They point out that conduit resonance is the cause of different spiral casing inlet pressure fluctuations. Fisher et al concludes in a similar way.

It would be desirable to be able to predict the dynamic pressure not only in the draft tube, but also in the vaneless space and the runner. Also, the ability to (ballpark) predict the strain in the runner by pressure measurement would be very welcome.

Based on measured model and prototype draft tube pressure, Fisher et al stated these relations:



$$\pm \hat{h}_p = \frac{H_p}{H_m} \cdot (\pm \hat{h}_m) \quad [\text{mWc}] \quad \text{Eq. 10}$$

$$f_p = \frac{f_{n_p}}{f_{n_m}} \cdot f_m \quad [\text{Hz}] \quad \text{Eq. 11}$$

These relations will be compared with the measured pressure data from the Tokke model and prototype measurements. The preliminary analysis shows a clear correlation between dynamic model and prototype draft tube pressure, as Fisher et al found. However, the Fisher pressure relation does not hold for the runner onboard dynamic pressure. Nor was any clear correlation between dynamic pressure and dynamic strain found. Still, this topic will be investigated further.

Lowys et al [23] performed onboard pressure and strain measurements, and found no significant correlation between dynamic pressure and strain in a low head Francis model runner. Strain measurements on the Andritz model runner for Tokke showed no significant stresses in the runner. This is explained in Chapter 5.2.

## **7.2 Comparison of conventional and splitter blade design**

For the Tokke model test stand, one conventional model runner and one splitter blade model runner was tested. It is of general interest to investigate the difference in onboard dynamic pressure between the two runner designs. Such studies might be performed during a post-doc continuation of the work presented in this thesis.

## **7.3 Strain measurement analysis**

Strain measurements can give an indication of which operating points that induce the worst stress conditions in the runner blades. A procedure that can be used is as follows:

1. Rainflow cycle counting method. This method results in a matrix representing the irregular time series as various combinations of range, frequency and mean [54].
2. The results from the Rainflow cycle counting method can be inserted into the Basquins law, to calculate the reduced lifetime resulting from each range, frequency and mean.
3. Then these data can be used in the Palmgren-Miner rule, to calculate the reduction of lifetime of the runner blade.

Performing this procedure for all operating points and strain gauges, will be time consuming. The results can be very interesting regarding the lifetime estimation of the runner; however this must be left for further work due to thesis time constraints.



## 8 Bibliography

[1] Coutu, A., Proulx, D., Coulson, S., and Demers, A., 2004, "Dynamic Assessment of Hydraulic Turbines", *Hydrovision 2004*, Montreal, Canada.

[2] Åril, B., 2009, "Sønnå Høy - Runner Breakdown (in Norwegian)", *Produksjonsteknisk Konferanse*, Gardermoen, Norway.

[3] Trønderenergi, 2008, Løpehjulet I Driva Løper Ikke Lenger, Accessed 15th May 2009, [http://web2054.increo.no/uploads/dokumenter/PDF/Lyspunktet/Lyspunktet1\\_08\\_web.pdf](http://web2054.increo.no/uploads/dokumenter/PDF/Lyspunktet/Lyspunktet1_08_web.pdf)

[4] Vu, T. C., and B.Nennemann, 2006, "Modern Trend of Cfd Application for Hydraulic Design Procedure ", Proceedings from the 23rd IAHR Symposium Yokohama, Japan, Isbn 4-8190-1809-4

[5] Rheingans, W. J., 1940, "Power Swings in Hydroelectric Power Plants ", Transaction of the ASME, Vol 62, pp 171-184.

[6] Falvey, H. T., 1993, "A Primer on Draft Tube Surging ", Hydro Review, Iss. February, pp 76-86.

[7] Wedmark, A., 1994, "Alleviating Pulsations in Turbines ", Hydro Review, Iss. October, pp 62-69.

[8] Kjeldsen, M., Dahlhaug, O. G., Nielsen, T. K., and Olsen, K. M., 2006, "Water Injection for the Mitigation of Drafftube Pressure Pulsations ", Proceedings from the IAHR Int. Meeting of WG on Cavitation and Dynamic Problems in Hydraulic Machinery and Systems, Barcelona, Spain.

[9] Susan-Resiga, R., Vu, T. C., Muntean, S., Ciocan, G. D., and Nennemann, B., 2006, "Jet Control of the Draft Tube Vortex Rope in Francis Turbines at Partial Discharge", Proceedings from the 23rd IAHR Symposium, Yokohama, Japan, Isbn 4-8190-1809-4

- [10] Qian, Z.-D., Yang, J.-D., and Huai, W.-X., 2007, "Numerical Simulation and Analysis of Pressure Pulsation in Francis Hydraulic Turbine with Air Admission", *Journal of Hydrodynamics*, Ser. B, Vol 19, Iss. 4, pp 467-472.
- [11] Francke, H. H., 2010, "Increase of Area of Operation and Efficiency for Water Turbines with Water Injection in the Draft Tube", PhD Thesis, Department of Energy and Process Engineering, Norwegian University of Science and Technology, Trondheim.
- [12] Avellan, F., 2006, "Flow Investigation in Draft Tube". Eureka Project No 1625, Accessed 19.02.2010, <http://lmhdb.epfl.ch/flindt.html>
- [13] Farhat, M., 2004, Hydrodyna Homepage: Harnessing the Dynamic Behavior of Hydro Turbines, Storage Pumps and Pump-Turbines, Accessed 19.02.2010, <http://lmhdb.epfl.ch/hydrodyna.html>
- [14] Ciocan, G. D., Iliescu, M. S., Vu, T. C., Nennemann, B., and Avellan, F., 2007, "Experimental Study and Numerical Simulation of the Flindt Draft Tube Rotating Vortex", *Journal of Fluids Engineering-Transactions of the Asme*, Vol 129, Iss. February, pp 146-158.
- [15] Keck, H., and Sick, M., 2008, "Thirty Years of Numerical Flow Simulation in Hydraulic Turbomachines", *Acta Mechanica*, Springer Verlag, Vol 201, Iss. 1, pp 211-229.
- [16] Stein, P., 2007, "Numerical Simulation and Investigation of Draft Tube Vortex Flow", Thesis, Coventry University, Coventry, UK.
- [17] Ghidaoui, M. S., Zhao, M., Mcinnis, D. A., and Axworthy, D. H., 2005, "A Review of Water Hammer Theory and Practice", *Applied Mechanics Review*, Vol 58, Iss. January, pp 49-75.
- [18] Ausoni, P., Farhat, M., Bouziad, Y. A., Kueny, J.-L., and Avellan, F., 2006, "Kármán Vortex Shedding in the Wake of a 2d Hydrofoil: Measurements and Numerical Simulation", *IAHR Int. Meeting of WG on Cavitation and Dynamic Problems in Hydraulic Machinery and Systems*, Barcelona, Spain.

- [19] Farhat, M., Natal, S., Avellan, F., Paquet, F., Lowys, P., and Couston, M., 2002, "Onboard Measurements of Pressure and Strain Fluctuations in a Model of Low Head Francis Turbine. Part 1: Instrumentation ", *Proceedings of the XXIst IAHR Symposium on Hydraulic Machinery and Systems*, Lausanne, Switzerland.
- [20] Lowys, P., Paquet, F., Couston, M., Farhat, M., Natal, S., and Avellan, F., 2002, "Onboard Measurements of Pressure and Strain Fluctuations in a Model of Low Head Francis Turbine. Part 2: Measurements and Preliminary Analysis Results ", *Proceedings of the XXIst IAHR Symposium on Hydraulic Machinery and Systems*, Lausanne, Switzerland.
- [21] Avellan, F., Etter, S., Gummer, J. H., and Seidel, U., 2002, "Dynamic Pressure Measurements on a Model Turbine Runner and Their Use in Preventing Runner Fatigue Failure ", *Proceedings of the The XXIst IAHR Symposium on hydraulic machinery and systems*, Lausanne, Switzerland.
- [22] Farhat, M., Avellan, F., and Seidel, U., 2002, "Pressure Fluctuation Measurements in Hydro Turbine Models ", *Proceedings from the The 9th International Symposium on Transport Phenomena and Dynamics of Rotating Machinery*, Honolulu, Hawaii, US.
- [23] Lowys, P. Y., Deniau, J. L., Gaudin, E., Leroy, P., and Djatout, M., 2006, "On-Board Model Runner Dynamic Measurements ", *Proceedings from the HydroVision 2006*, Portland, Oregon, US.
- [24] Bjørndal, H., Moltubakk, T., and Aunemo, H., 2001, "Flow Induced Stress in a Medium Head Francis Runner ", *10th International Meeting of the Work Group on The behaviour of hydraulic machinery under steady oscillatory conditions*, Trondheim, Norway.
- [25] Bjørndal, H., and Hofstad, Ø., 2002, "Start- Og Stoppkostnader for Vannkraftaggregater. Vedlegg 3: Strekkklappmålinger Av Spenninger I Løpehjulet under Drift," Technical Report No. EBL 85-2002, Norconsult, Oslo, Norway. (in Norwegian)
- [26] Lowys, P. Y., Doyon, J., Couston, M., and Vuillerod, G., 2001, "Dynamic Behaviour of Low Head Francis Turbines", *10th international meeting of the work group on the behaviour of*

*hydraulic machinery under steady oscillatory conditions*, Trondheim, Norway.

[27] Dahlhaug, O. G., Storli, P. T. S., Ramdal, J., and Brandåstrø, B., 2007, "Tokke Model Test 2006-2007. NTNU Reference Runner," Technical Report. Norwegian University of Science and Technology, Trondheim.

[28] Alekseenko, S. V., Kuibin, P. A., Okulov, V. L., and Shtork, S. I., 1999, "Helical Vortices in Swirl Flow", *J. Fluid Mech*, Vol 382, pp 195-243.

[29] Wahl, T. L., Skinner, M. L., and Falvey, H. T., 1991, "The Twin Vortex Draft Tube Surge", *Waterpower*, Denver, CO, USA.

[30] Sayma, A. I., Vahdati, M., and Imregun, M., 2000, "An Integrated Nonlinear Approach for Turbomachinery Forced Response Prediction. Part I: Formulation", *Journal of Fluids and Structures*, Vol 14, Iss. 1, pp 87-101.

[31] Nicolet, C., Ruchonnet, N., and Avellan, F., 2006, "One-Dimensional Modeling of Rotor Stator Interaction in Francis Pump-Turbine", *Proceedings from the 23rd IAHR Symposium*, Yokohama, Japan, Isbn 4-8190-1809-4

[32] Brennen, C. E., 1994, *Hydrodynamics of Pumps*, Concepts ETI, Inc and Oxford University Press, Isbn 0-933283-07-5, 0-19-856442-2

[33] Larsson, C., 2003 "Experimental and Theoretical Analysis of Inlet Flow of Francis Turbine Runner", Dr.Ing. Thesis, Department of Energy and Process Engineering, Norwegian University of Science and Technology, Trondheim, Norway.

[34] Blanco, E., Parrondo, P., Barrio, R., Gonzales, J., Santolaria, C., and Fernandez, 2006, "Fluid Dynamic Radial Forces at the Blade Passing Frequency in at Centrifugal Pump with Different Impeller Diameters ", *IAHR Int. Meeting of WG on Cavitation and Dynamic Problems in Hydraulic Machinery and Systems*, Barcelona, Spain.

[35] Jernsletten, J., 1995, "Analysis of Non-Stationary Flow in a Francis Reversible Pump Turbine Runner", Dr.Ing. Thesis, Division

of Thermal Energy and Hydropower, The Norwegian Institute of Technology, The University of Trondheim, Trondheim, Norway.

[36] Stepanik, H. E., 1991, "Reversible Francis Pump-Turbines: Improvement of Part Load Performance by Changes on the Design of Impeller Blades", Dr.Ing. Thesis, Department of Hydro and Gas Dynamics, Faculty of Mechanical Engineering, The Norwegian Institute of Technology, The University of Trondheim, Trondheim.

[37] Stücker, A., 2007, "Cfd-Analysis of the Stay Vanes in a High Head Francis Turbine", Diploma Thesis, Department of Energy and Process Engineering, Norwegian University of Science and Technology, Trondheim, Norway.

[38] Kumar, P., and Saini, R. P., "Study of Cavitation in Hydro Turbines - a Review", *Renewable and Sustainable Energy Reviews*, Vol 14, Iss. 1, pp 374-383.

[39] Kjeldsen, M., 1999, "Cavitation in Hydraulic Machinery", Dr.Ing. Thesis, Department of Energy and Process Engineering, Norwegian University of Science and Technology, Trondheim.

[40] White, F. M., 1999, *Fluid Mechanics*, McGraw-Hill, Isbn 0-07-116848-6

[41] Sick, M., Michler, W., Weiss, T., and Keck, H., 2009, "Recent Developments in the Dynamic Analysis of Water Turbines", *Journal of Power and Energy*, Vol 223, Iss. JPE578.

[42] Vu, T. C., Nennemann, B., Ausoni, P., Farhat, M., and Avellan, F., 2007, "Unsteady Cfd Prediction of Von Kármán Vortex Shedding in Hydraulic Turbine Stay Vanes", *Hydro 2007*, Granada, Spain.

[43] Lockey, K. J., Keller, M., Sick, M., Staehle, M. H., and Gehrler, A., 2006, "Flow Induced Vibrations at Stay Vanes: Experience at Site and Cfd Simulation of Von Kármán Vortex Shedding", *Hydro 2006*, Porto Carras, Greece.

[44] Zobeiri, A., Ausoni, P., Avellan, F., and Farhat, M., 2009, "Vortex Shedding from Blunt and Oblique Trailing Edge Hydrofoils", *Proceedings from the 3rd IAHR International Meeting of the Workgroup on Cavitation and Dynamic Problems in Hydraulic Machinery and Systems*, Brno, Czech Republic.



- [45] Wheeler, A. J., and Ganji, A. R., 2004, *Introduction to Engineering Experimentation*, Pearson Prentice Hall, Isbn 0-13-124685-2
- [46] Press, W. H., Teukolsky, S. A., Vetterling, W. T., and Flannery, B. P., 2007, *Numerical Recipes: The Art of Scientific Computing*, Cambridge University Press, Isbn 978-0-521-88068-8
- [47] Kobro, E., Dahlhaug, O. G., and Nielsen, T., 2008, "Onboard Pressure Measurements in Francis Model Runner Blades", Proceedings from the 24th IAHR Symposium on Hydraulic Machinery and Systems, Foz Do Iguazzu, Brazil, ISBN 978-85-60858-13-1
- [48] Antonsen, Ø., 2007, "Unsteady Flow in Wicket Gate and Runner with Focus on Static and Dynamic Load on Runner", PhD Thesis, Department of Energy and Process Engineering, Norwegian University of Science and Technology, Trondheim, Norway.
- [49] Siwani, Y. D., 2008, "Dynamic Stress Assessment in High Head Francis Runners", Master Thesis, Department of Applied Physics and Mechanical Engineering, Luleå University of Technology, Luleå, Sweden.
- [50] Dörfler, P., 1984, "On the Phase Resonance in Vibrations Caused by Blade Passage in Radial Hydraulic Turbomachines", Proceedings from the The 12th IAHR Symposium, Stirling, UK.
- [51] Iec 60193, "Hydraulic turbines, storage pumps and pump-turbines - Model acceptance tests. 2nd edition", 1999, International Electrotechnical Commission
- [52] Jacob, T., Prenat, J. E., Perusset, C., Buffet, G., Avellan, F., and Chapuis, L., 1996, "Pressure Fluctuations of Francis Turbines: Model and Prototype Test Results", Proceedings from the Proceedings of Modelling, Testing and Monitoring for Hydro Powerplants II, Lausanne, Switzerland.
- [53] Fisher, R. K., Palde, U., and Ulith, P., 1980, "Comparison of Draft Tube Surging of Homologous Scale Models and Prototype Francis Turbines", *10th IAHR Symposium*, Tokyo, Japan.

- [54] Dowling, N. E., 2007, *Mechanical Behaviour of Materials. Engineering Methods for Deformation, Fracture and Fatigue*, Pearson Prentice Hall, Isbn 0-13-186312-6
- [55] Haaks, M., and Maier, K., 2006, *Predicting the Lifetime of Steel, Extreme Events in Nature and Society*, Springer Berlin Heidelberg, Isbn 978-3-540-28610-3
- [56] Bathias, C., 1999, "There Is No Infinite Fatigue Life in Metallic Materials", *Fatigue Fract Engng Mater Struct*, Vol 22, pp 559-565.
- [57] Bathias, C., Drouillac, L., and Le Francois, P., 2001, "How and Why the Fatigue S-N Curve Does Not Approach a Horizontal Asymptote", *International Journal of Fatigue*, Vol 23, pp S143-S151.
- [58] Bathias, C., and Paris, P. C., 2005, *Gigacycle Fatigue in Mechanical Practice*, Marcel Dekker, New York, Isbn 0-8247-2313-9
- [59] Marines, I., Bin, X., and Bathias, C., 2003, "An Understanding of Very High Cycle Fatigue of Metals", *International Journal of Fatigue*, Vol 25, Iss. pp 1101-1107.
- [60] Miller, K. J., and O'donnell, W. J., 1998, "The Fatigue Limit and Its Elimination", *Fatigue Fract Engng Mater Struct*, Vol 22, pp 545-557.
- [61] Kanazawa, K., and Nishijima, S., 1997, "Fatigue Fracture of a Low Alloy Steel in the Ultra-High Cycle Region under Elevated Temperature Conditions", *J. Japan Soc. Mater. Sci.*, Vol 46.



## **9 Appendices**

### **9.1 Appendix 1 – Summary of Paper 5**

Kobro, E., Gamboa, A., Fjærvold, K.T., 2009, “A successful cooperation between a power company a turbine manufacturer and a university”, Hydro 2009, Lyon, France.

This paper describes the cooperation between Andritz Hydro, Statkraft and NTNU. As Statkraft decided to refurbish several high head Francis units, Andritz won the tender process. NTNU was chosen as the neutral test facility. By including the university in the model efficiency measurements, possibilities for elaborate research on the Tokke model and prototype runners opened up.

The paper was written as a non-technical paper for the Hydro 2009 conference, to inform about the possibilities the cooperation resulted in.

## 9.2 Appendix 2 - A brief discussion on high cycle fatigue

Fatigue and fatigue limits are unavoidable topics when discussing life time of mechanical components subjected to cyclic loads. The behaviour of the materials of the turbine has not been a focus in this work. However, it has been noted that new research results advocate a new understanding of fatigue limits, and state that the limits not necessarily appear as reported from previous research. This new research is only briefly described here.

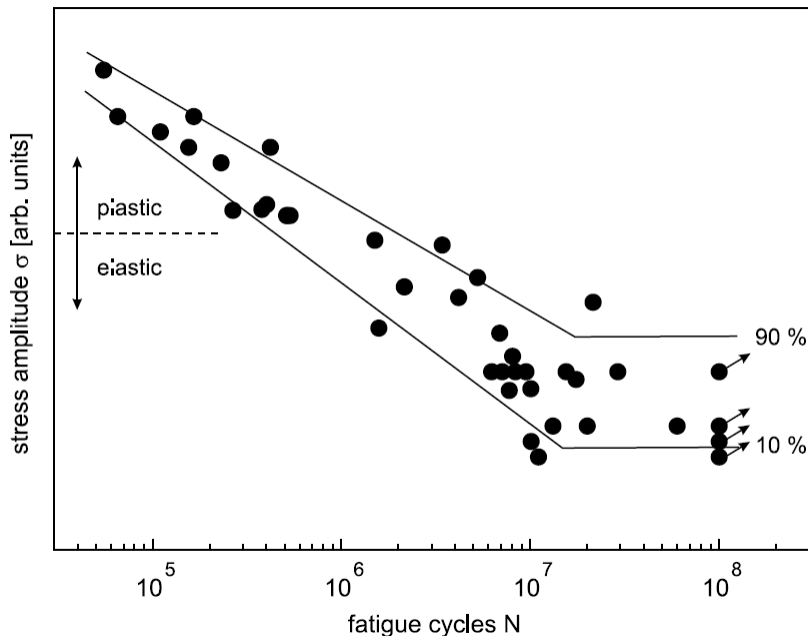


**Figure 9-1. Schematic example of classical Wöhler curve, indicating a fatigue limit appearing at approx.  $10^7$  cycles [55]. The upper (lower) line indicate 90% (10%) probability of failure at a given stress amplitude.**

The Wöhler curves (S/N curves) play a key role, a typical example is shown in Figure 9-1. However, the traditional understanding of these curves is now challenged. Authors such as Bathias [56-58], Marines [59] and Miller [60] claim the S/N curves do not approach a horizontal asymptote, independent of initial crack size. Dowling

[54], Bathias and Miller has published papers advocating this paradigm. Miller discussed ferrous metals in general. Both Marines and Bathias investigated 17-4PH martensitic steel, cast iron, low carbon steel, and spring steel. Bathias also investigated 12Cr martensitic steel, SS 304 and 4240 CroMo steel (for chemical composition of the materials, see the referenced articles).

Their claim is that the S/N curve does not have a tangential threshold limit for numbers of cycles above a certain limit, in the so-called gigacycle regime ( $10^9$  number of cycles and above). This results in the removal of the so-called infinite fatigue life. At a very high number of cycles and at certain R-values, intercrystalline processes will cause cracks to propagate, even with relatively low stress amplitudes. In Figure 9-2, the declining S/N curve for martensitic steel is shown. In Figure 9-3, the S/N curve for 1Cr-0.5Mo steel for different temperatures is shown. Here it appears that there is a temporary threshold up to a certain number of cycles, until the curves continue to decline.

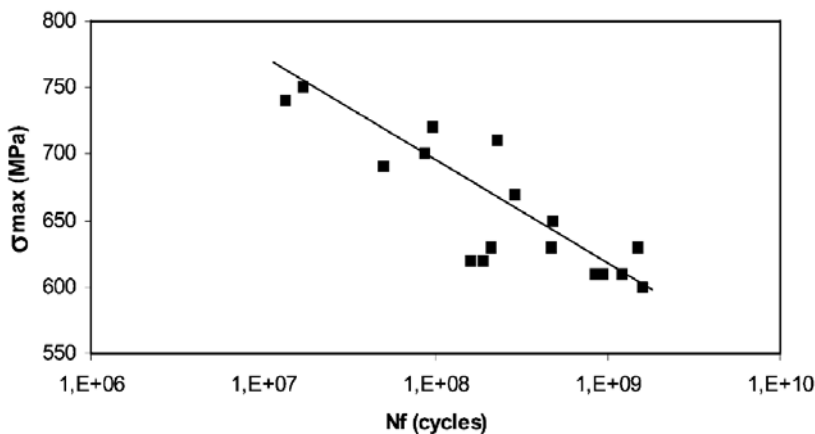
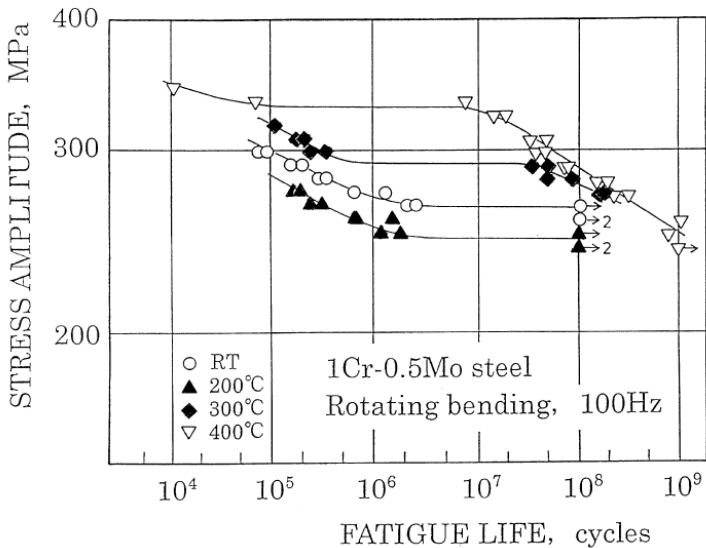


Figure 9-2. S/N curve for 17-4PH martensitic stainless steel, showing no threshold above  $10^7$  cycles [59].



**Figure 9-3. S/N curve for 1Cr-0.5Mo steel at different temperatures [61]. Note that the tests at room temperature indicate a threshold up to  $10^8$  cycles.**

Using Tokke as an example, the highest rotor stator interaction frequency is 175 Hz, and the unit would have to operate for more than 30 years to reach  $10^{11}$  cycles. Hence, most Francis units will experience such high number of cycles at the end of their life time. However, when there is still not clear how the S/N curves actually develops, and when fatigue still is a problem, the direction of fatigue research needs to be given significant attention.

Dowling [54] also performed a somewhat modified fatigue test that can be relevant for this discussion. The test specimen was subjected to the normal cyclic loading of such tests. In addition to this, one cycle with higher strain amplitude was applied at every  $10^5$  cycle. This larger amplitude was well within the yields strength of the test specimen. This test resulted in a quite different S/N curve. The slope did not flatten towards a horizontal threshold value as for traditional S/N curves, it continued with approximately the same slope when moving from lower number of cycles to a higher number of cycles. The addition of this strain irregularity can be described as a more realistic strain situation, because industrial components always experience variable load conditions. An example of such from a Francis turbine is the start or stop

sequence, where the runner and other components can be subjected to a limited number of higher strain amplitudes for short periods of time. Also, during operation, a turbine will experience start and stop cycles. These are relatively rare cycles, but do result in large amplitudes.

In addition to fatigue, a likely cause of the so-called shark bite fatigue failures are that the design process has evolved so far that the mechanical integrity has unwittingly been sacrificed when striving to optimize hydraulic efficiency. The tools for dynamic CFD and FEM simulations and the coupling between them are still evolving. Because of this, the effect of the hydraulic dynamic loads may not have been calculated at a sufficient degree of accuracy. The results may have been interpreted in a manner that has indicated strain well within safety limits, even if the total dynamic strain experienced during operation is above the allowable safety limits.



### 9.3 Appendix 3 - The model test rig

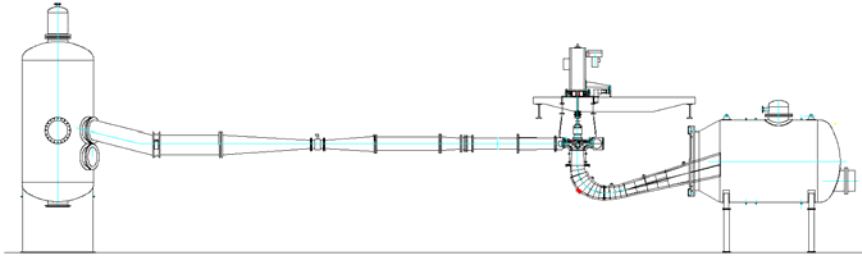


**Figure 9-4. Francis test rig**

The Francis rig at the Waterpower Laboratory at NTNU consists of a reservoir, two pumps, a pressure tank, the turbine with draft tube, a suction tank and connecting pipes. The rig can be operated as open or closed loop, suction tank absolute pressure can be controlled and content of non-dissolved air can be monitored.

The overall specification of the test rig is as follows:

Pump power:	2 · 330kW
Generator power:	130 kW
Water reservoir:	450 m <sup>3</sup>
Maximum head:	100mWc

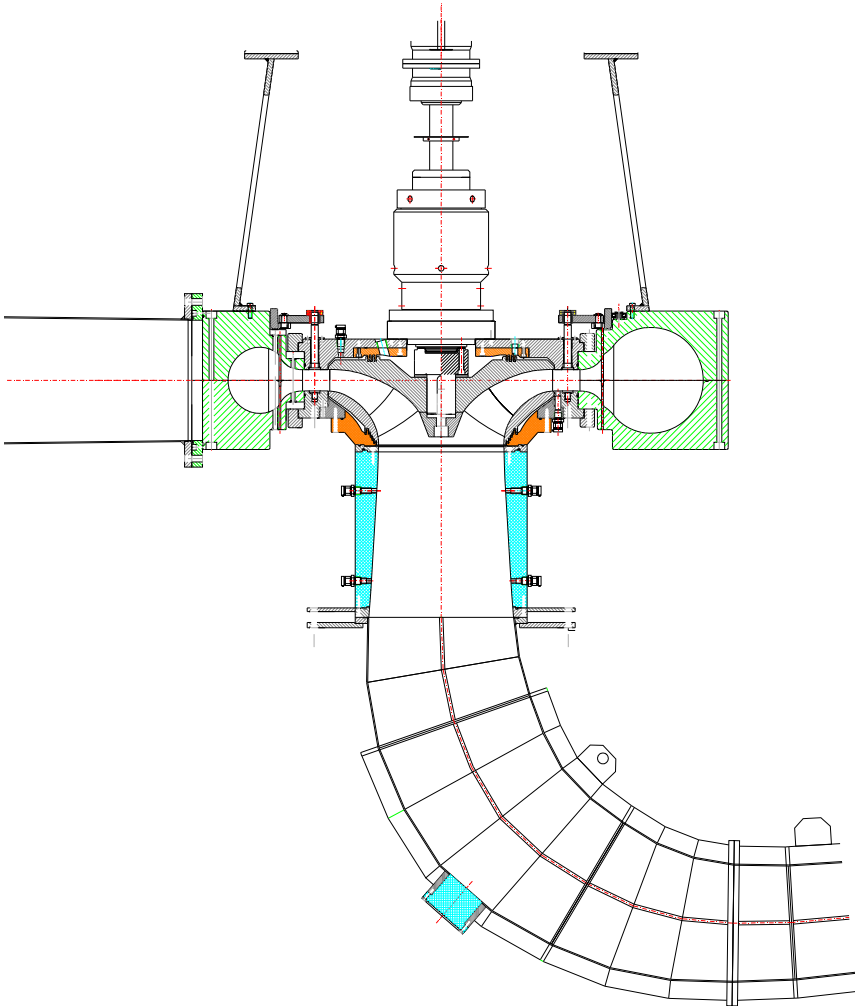


**Figure 9-5. Cross section of the model turbine, with the NTNU splitter blade model runner installed.**

## 9.4 Appendix 4 - Pictures of the draft tube vortex

Best efficiency point of the turbine was at  $n_{ED}=0.18$  and  $q_{ED}=0.153$ , at a guide vane opening of  $\alpha = 10^\circ$ .



Figure 9-6.  $n_{ED}=0.205$ ;  $q_{ED}=0.058$ ;  $\alpha=4^\circ$ . Extreme part load

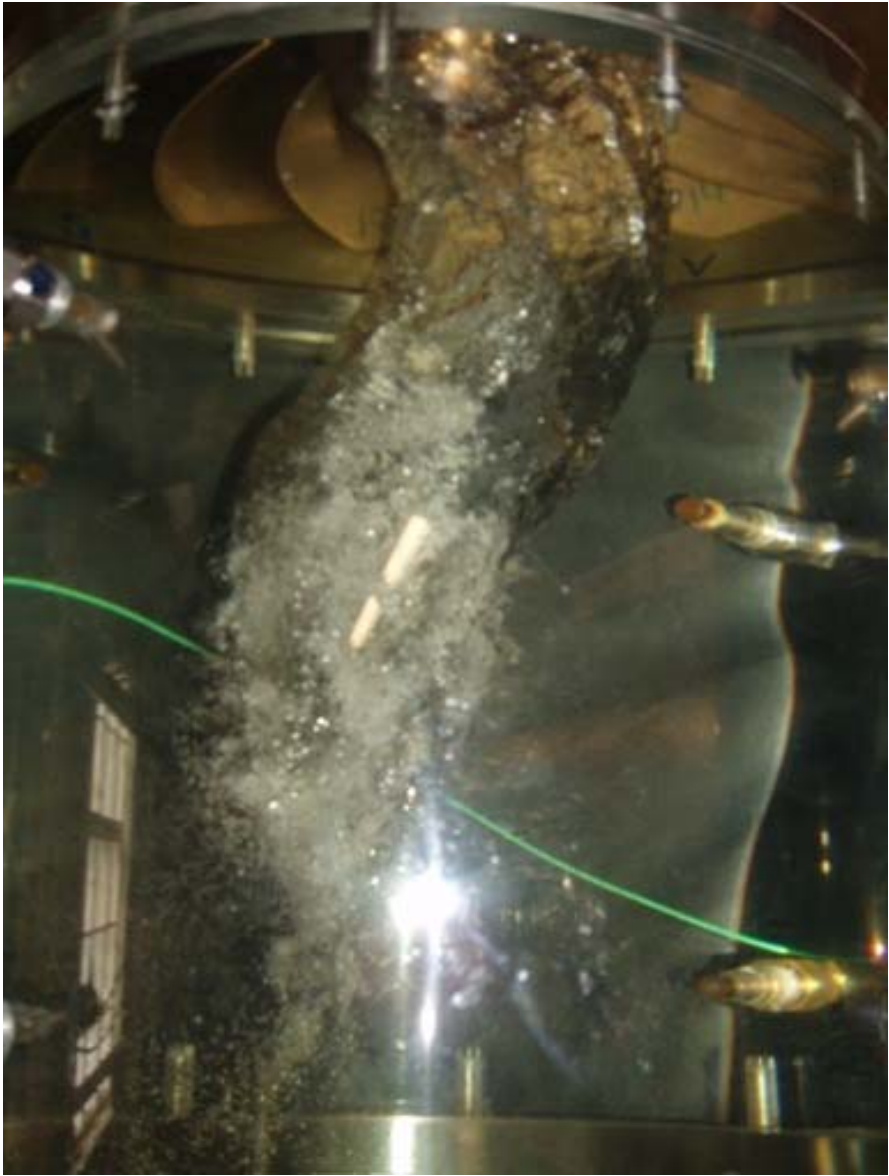


Figure 9-7.  $n_{ED}=0.205$ ;  $q_{ED}=0.1$ ;  $\alpha=7^\circ$ . Part load



Figure 9-8.  $n_{ED}=0.165$   $q_{ED}=0.175$ ,  $\alpha=11^\circ$ . Overload



Figure 9-9.  $n_{ED}=0.15$   $q_{ED}=0.22$ ,  $\alpha=14^\circ$ . Extreme over load



## **Part 2 - Papers**





## **PAPER 1**

*Kobro, E., Dahlhaug, O. G., and Nielsen, T., 2008, "Onboard Pressure Measurements in Francis Model Runner Blades", Proceedings from the 24th IAHR Symposium on Hydraulic Machinery and Systems, Foz Do Iguazzu, Brazil, ISBN 978-85-60858-13-1.*



# ONBOARD PRESSURE MEASUREMENT IN FRANCIS MODEL RUNNER BLADES

## AUTHORS

PhD Candidate Einar Kobro

Professor Ole G. Dahlhaug

Professor Torbjørn K. Nielsen

Norwegian University of Science and Technology (NTNU)

Waterpower Laboratory

Alfred Getz vei 4, 7491 Trondheim, Norway

Phone: +47 47608861, Fax: +47 73 59 38 54

[einar.kobro@ntnu.no](mailto:einar.kobro@ntnu.no)

## ABSTRACT

The empirical scale-up relations from model to prototype values for efficiency measurements on hydro turbines are known. There is a desire to develop a similar scale-up possibility for pressure pulsation levels. Alongside the refurbishment project on Tokke hydro power plant in Telemark, Norway, two model and two prototype Francis runners have been made accessible for onboard pressure measurements.

There was developed two different model runners during the project, both designed to fit in a 5:1 scaled down spiral casing of the existing Tokke turbine. At Norwegian University of Science and Technology (NTNU), a model runner was designed and manufactured, to function as a reference runner in the NTNU test rig. The supplier of the replacement runners, Andritz VA Tech Hydro, tested their model runner in the same rig.

Miniature strain gauge based pressure sensors were mounted in the blade surface of both runners. The cables were run through the thrust bearing, and connected to a wireless telemetry transmitter on the shaft. This setup enabled high speed measurement of the static and dynamic pressure development on the

runner blades. Due to the geometry of Francis runner blades, placing the sensors without altering the channel geometry and preventing leakages was a challenge. However, this proposed setup worked as intended.

**KEY WORD:** Francis model turbine, onboard pressure pulsation measurements

## INTRODUCTION

Modern power plants are often operated under off-design conditions. These operating patterns results in dynamic pressure fluctuations which induces increased vibrations and noise in the turbine. These conditions exert large stresses on the turbine components, which might ultimately lead to fatigue failure. Therefore, gaining a deeper knowledge of the pressure development in the turbine is an important topic for the hydro power industry. It is desirable to be able to predict prototype pressure development from model tests. However, a general scale-up relation does not exist.

Statkraft is the owner of Tokke hydro power plant in Southern Norway. The plant consists of 4 units of 110MW each, built in 1961. The rated head is 377 meters, and the speed number of the turbine is 0.27. The runners were produced by Kværner Brug, with 15+15 splitter blade design. Statkraft decided to refurbish the plant, and VA Tech was assigned the delivery of replacement runners. These new runners will have 17 blades.

The model tests of the VA Tech runner were performed in The Waterpower Laboratory at Norwegian University of Science and Technology (NTNU). To ensure proper repeatability of the test rig, an additional runner was designed as a reference runner. This runner was of 15+15 splitter blade design.

Both model runners have been made accessible for onboard pressure measurement. They will be instrumented with miniature strain gauge based pressure sensors, milled down into the blade surface. The signals will be transmitted by a telemetry system mounted on the turbine shaft.

A similar test setup was developed in the EPFL environment (Refs 1-4). In these tests, miniature pressure transducers were manufactured in-blade. All electronic signal conditioning and storage was done in the runner crown and on

the shaft. In Ref 5, Farhat et al mounted accelerometers in a low head Francis prototype. In Refs 1-5, onboard signal conditioning electronics connected to a slip ring connection has been used. In the test setup described in this article, digital wireless telemetry transmission has been used instead of slip rings, reducing the risk of high frequency noise.

To contribute to a discussion regarding such an empirical relation, the pressure in two model and prototype runners will be measured. In October 2008, the first of four new prototype runners will be delivered from Andritz VA Tech Hydro to the plant. Both the existing Kværner Brug runner and the Andritz VA Tech Hydro replacement runners will be instrumented with pressure sensors in the blade surface.

The future investigation will look into how known frequencies such as blade passing frequency and draft tube vortex frequency propagate through the model and prototype runners.

This article presents the setup for onboard pressure measurements on the model runners, and preliminary measurement results verifying the reliability of the setup. Future articles will present: 1) the analyzed results from the lab measurements of the two different model runners, 2) the prototype setup and analyzed results of the two different prototype runners, and finally 3) a discussion of an empirical scale-up relation of the static and dynamic pressure development. Future work will include comparison with transient CFD.

## **METHODOLOGY**

When deciding on the placement of the sensors, the main objective was to facilitate future comparison between the two model runners and the two prototype runners. Three stream lines were chosen; one close to the hub, one at the middle of the channel, and one close to the ring. One sensor was placed on each stream line close to the inlet, and one close to the outlet. On the NTNU splitter blade model, one sensor was placed just upstream the splitter blade outlet, and one just downstream the splitter blade outlet. On the VA Tech model, sensors were placed in the same relative position as the sensors downstream the splitter blade outlet on the NTNU runner.

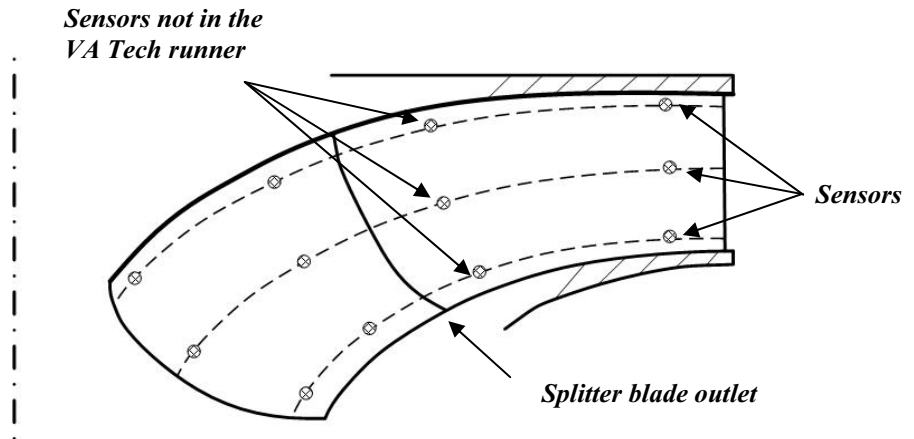


**Figure 1 – Schematic view of sensor placement in NTNU runner. Four sensors were placed on each of the three stream lines**

It was of great importance that the sensors would not disturb the flow through the hydraulic channel. Because of the geometry of Francis model runner blades, the sensors needed to be of very small physical size. The sensor chosen was Kulite LL080, a miniature Wheatstone full bridge sensor. The thickness of the sensor is only 1.53mm. This made it possible to mill down grooves in the blade, also at the blade outlet. The sensors were attached to a given position using a flexible silicone adhesive, to reduce the influence from structural vibration of the blade on the sensor. Then the cables were covered with epoxy, see Figure 2 and Figure 3. After curing, the epoxy was grinded off, leaving a smooth surface. Finally the epoxy was coated with a thin coating agent. This reduced the surface roughness of the epoxy, and ensured a smooth surface around the sensor and over the cables. The cables were then taken out of the blade, through the hub, into the shaft and finally out of the shaft into atmospheric pressure above the thrust bearing. In the NTNU runner, a total of 25 sensors were mounted in the blades, and in the VA Tech model runner a total of 18 sensors were mounted.

A brief procedure for installation follows:

1. Defining the sensor placement.
2. Milling notches for sensors and cables
3. Fixing sensors at correct height using silicone adhesive.
4. Covering sensors and cables with epoxy, and curing epoxy.
5. Grinding off excessive epoxy to a smooth surface.

6. Coating the epoxy surface to reduce surface roughness.
7. Ensuring water tight cable passages.



**Figure 2 – Pressure transducers in the NTNU runner, during installation.**



**Figure 3 – Finished installation (left), and during installation (right).**





**Figure 4 - Installing the instrumented NTNU runner. The cables from the sensors are run through the shaft.**

### **Telemetry system**

There are several wireless telemetry systems commercially available. Some of these are versatile and heavy systems, others are small in size but of less versatility and with a lower bit rate. The system chosen was a Summation Research SRI-500e system. This system is highly versatile, but still small and light weight in physical size, and very robust. The system configuration chosen enabled simultaneous logging of four full bridge channels at 2.1kHz at 16 bit. The signals were multiplexed, compensated for transmitter temperature, and the

carrier frequency from the transmitter was in the 869MHz range. In the receiver, the signals were amplified from 0-45mV to  $\pm 10V$ . Since all storage is done directly on the logging pc, there are virtually no limitations in memory depth.

### Sensors in stationary turbine parts

Sensors were also placed in stationary parts of the turbine. 3 sensors were placed in the rotational cavity, and up to six sensors in the draft tube cone. To be able to correlate the time series from the runner sensors and the stationary sensors, absolute time down to 100 microseconds were stored in the logging file. Also, an optical sensor gave a voltage burst at one defined angular position of the runner, to be able to monitor the runner rotation.

### Calibration

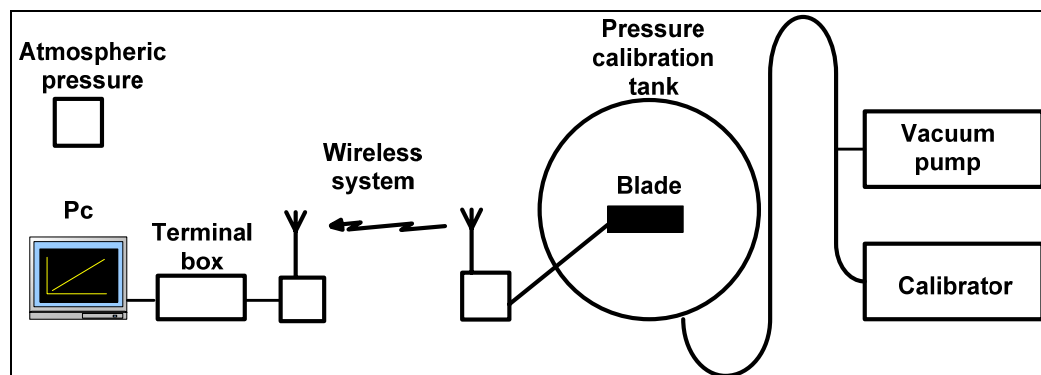
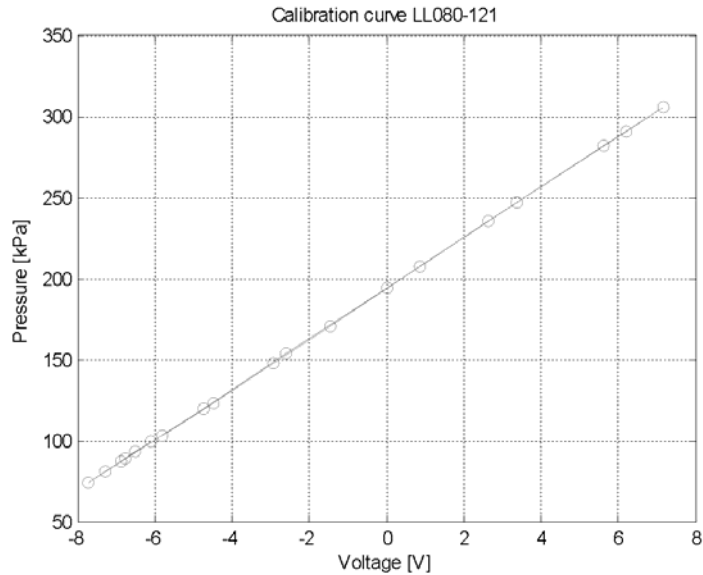


Figure 5 - Calibration setup

Static calibration of the instrumented blades were performed using the setup described in Figure 5. A vacuum pump was used to lower the pressure below atmospheric pressure. Dynamic calibration was considered not necessary, due to the fact that the sensors typically have a 300 kHz natural frequency.



**Figure 6 - Typical calibration curve**

## RESULTS

The system has proved to function well. Examples of the logging results are shown in Figure 7. In post processing, the time series are plotted and inspected. Then the time series are analyzed using the Power Spectral Density method in Matlab. Also, the standard deviation for each time series is computed. In Figure 7, time series and frequency analysis are plotted, at an operational point close to Best Efficiency Point. Sensor number 114 is placed at blade inlet, Sensor number 120 before splitter blade outlet, and Sensor number 130 at full blade outlet. The blade passing frequency of the turbine is 252Hz, which can clearly be seen from all three sensors. The dampening of the blade passing frequency through the channel is evident. In Figure 8, a shorter time window is displayed, to clearly display the blade passing frequency.

Wireless test number 8, n=540, ned=0.1829, qed=0.1368, gvo=9deg

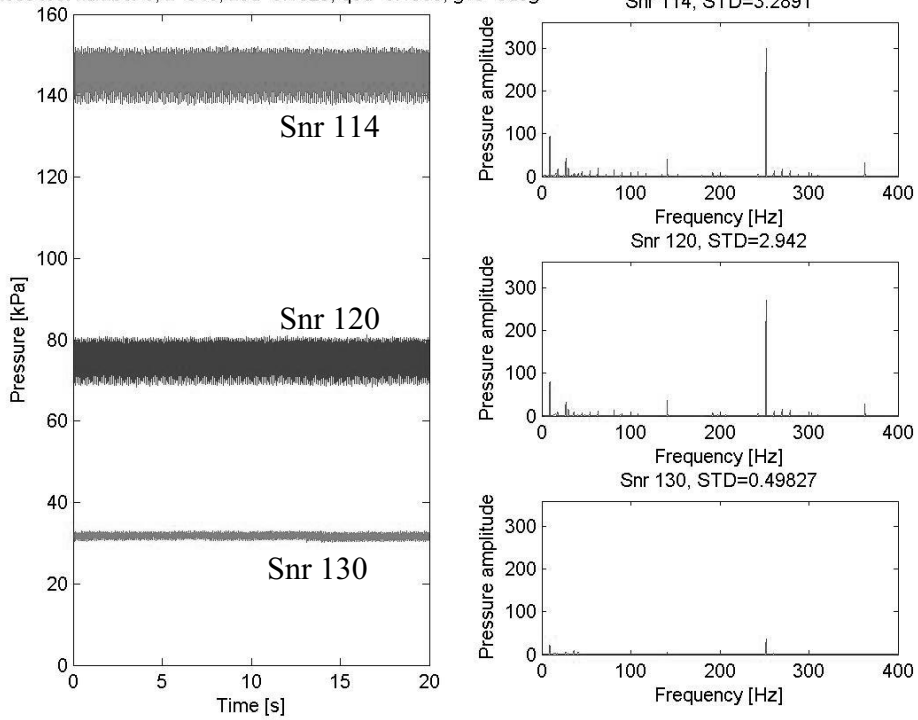


**Figure 7 - Time series and frequency analysis, close to Best Efficiency Point.**

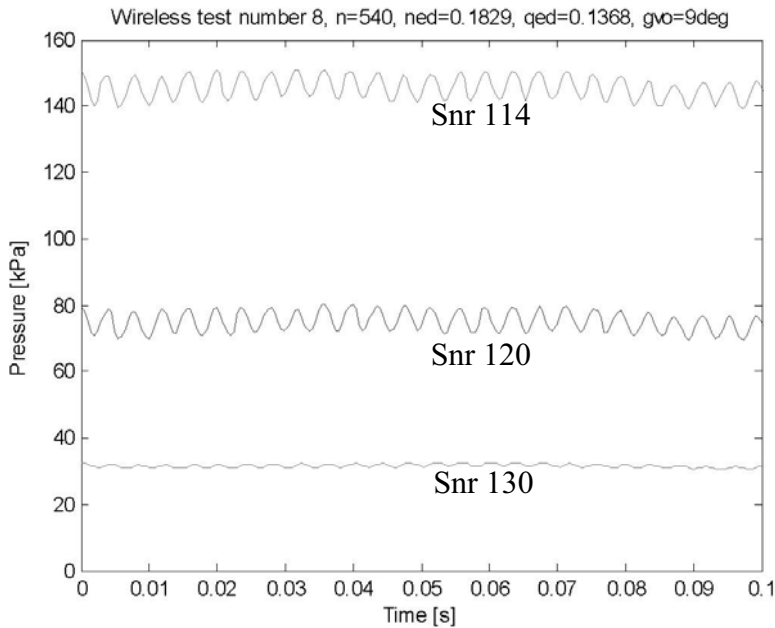


**Figure 8 - Time series in short time window, with blade passing frequency visible.**

The combined non-linearity, hysteresis and repeatability uncertainty of the sensors are typically  $\pm 0,1\%$  of full scale output,  $\pm 0,5\%$  at maximum.

One concern with the proposed setup is the durability of the sensors. Some sensors were lost during testing. It is therefore of great importance to ensure no water leakage into the sensors.

### **FINAL CONSIDERATIONS**

The logging system presented in this paper will create a good base for the model measurements needed for a future comparison with prototype onboard measurements. Preparing this setup is time consuming and costly, however it can be used as a guideline for other kinds of measurements in rotating machinery. Due to costs and time consumption, the intention is not to implement this procedure for standard model tests.

### **Acknowledgements**

The authors would like to express their gratitude to Andritz VA Tech Hydro in Zürich, in particular Mr. Alphonse Gamboa, for their co-operational will and efforts in this project. If they had not made their model and prototype

runners available for measurements, the future scale effect discussion would be based on a much vaguer base.

### **BIBLIOGRAPHICAL REFERENCES**

- [1] M. FARHAT, F.AVELLAN, U. SEIDEL, February 2002. *Pressure fluctuation measurements in hydro turbine models*. The 9<sup>th</sup> International Symposium on Transport Phenomena and Dynamics of Rotating Machinery. Honolulu, Hawaii, USA.
- [2] M. FARHAT, S. NATAL, F. AVELLAN, F. PAQUET, PY. LOWYS, M. COUSTON, September 2002. *Onboard measurements of pressure and strain fluctuations in a model of low head Francis turbine. Part 1: Instrumentation*. Proceedings of the XXI<sup>st</sup> Symposium on Hydraulic Machinery and Systems. Lausanne, Switzerland.
- [3] PY. LOWYS, F. PAQUET, M. COUSTON, M. FARHAT, S. NATAL, F. AVELLAN, September 2002. *Onboard measurements of pressure and strain fluctuations in a model of low head Francis turbine. Part 1: Measurements and preliminary analysis results*. Proceedings of the XXI<sup>st</sup> Symposium on Hydraulic Machinery and Systems. Lausanne, Switzerland.
- [4] F. AVELLAN, S. ETTER, J.H. GUMMER, U. SEIDEL, August, 2000. *Dynamic pressure measurements on a model turbine runner and their use in preventing runner fatigue failure*. Proceedings of the XX<sup>th</sup> Symposium on Hydraulic Machinery and Systems. Charlotte, North Carolina, USA.
- [5] M. FARHAT, P. BOURDON, P. LAVIGNE, R. SIMONEAU, June 1997. *Hydrodynamic aggressiveness of cavitating flows in hydro turbines*. Proceedings of the 1997 ASME Fluids Engineering Division Summer Meeting. Vancouver, Canada.



## **PAPER 2**

*Kobro, E., Gamboa, A., Bloch, R., and Nielsen, T. K., 2009, "Onboard Pressure Measurement in High Head Francis Prototype Runners", Proceedings from the 3rd IAHR International Meeting of the Workgroup on Cavitation and Dynamic Problems in Hydraulic Machinery and Systems, Brno, Czech Republic, ISBN 978-80-214-3947-4.*





## ONBOARD PRESSURE MEASUREMENT IN HIGH HEAD FRANCIS PROTOTYPE RUNNERS

**Einar Kobro \***

Waterpower Laboratory, Norwegian University of Science and Technology,  
Norway

**Alphonse Gamboa**

Andritz Hydro AG, Zürich, Switzerland

**Reinhard Bloch**

Andritz Hydro AG, Zürich, Switzerland

**Torbjørn Nielsen**

Waterpower Laboratory, Norwegian University of Science and Technology,  
Norway

### ABSTRACT

The empirical scale-up relations from model to prototype values for efficiency measurements for hydro turbines are well described. There is a desire to develop a similar scale-up possibility for pressure pulsation levels in Francis turbines. Alongside the refurbishment project on Statkrafts Tokke hydro power plant in Telemark, Norway, two model and two prototype Francis runners have been made accessible for onboard pressure measurements. One model was designed at NTNU, with splitter blade design. The original prototype runner was designed and manufactured by Kværner, with splitter blades. The replacement prototype and its model were designed and manufactured by Andritz VA Tech.

#### *Tokke power plant*

Owner: Statkraft  
Commissioned 1961  
4 x 110MW  
Nominal head = 377m  
Nominal flow = 30 m<sup>3</sup>/s  
Rotational speed = 375rpm  
 $\Omega=0,27$   
 $n_q=24$

\* *Corresponding author:* Waterpower Laboratory, Norwegian University of Science and Technology, Alfred Getz vei 4, 7491 Trondheim, Norway, phone: +47 47 60 88 61, fax: +47 73 59 38 54, email: [enar.kobro@ntnu.no](mailto:enar.kobro@ntnu.no)

To be able to perform onboard measurements on the original prototype and the replacement prototype, a logging system needed to be designed. Simultaneous high frequency measurement of several channels was the key feature. To reduce the extent of permanent alteration the turbine components, telemetry was rejected and onboard storage was a chosen feature. The logging unit was installed in the runner cone.

To fully exploit the potential of the developed logging chain on the prototype replacement runner, it was decided to simultaneously measure both strain and pressure on the runner blade outlet, and pressure at the inlet pressure side of one blade. The authors installed three Quartz pressure sensors lowered into the pressure side of the blade inlet, six miniature bridge based pressure transducers at the blade outlet both on pressure and suction side, and 16 strain gauges on both pressure and suction side of the outlet of the blades. In addition, there were installed pressure sensors in stationary parts such as draft tube cone and lower cover surface.

The test on the replacement runner was performed in February 2009 on Tokke Unit 3, as a cooperation between Andritz, NTNU and Statkraft. The test on the original runner was performed in October 2008. This test failed, and will probably be repeated during the summer of 2010.

An overview of the logging chain used for the Tokke Unit 3 replacement runner prototype will be presented in this paper, along with some preliminary results from the analysis of the pressure and strain measurements (presented in relative values due to confidentiality).

## **Keywords**

Francis prototype runner, onboard measurements, dynamic pressure and strain

## **1. Introduction**

In hydro power production, runner failure due to fatigue cracking is a problem of increasing relevance. The market demand enforces operation of hydro units on a wider load range and with more frequent starts and stops. The desire for higher efficiencies results in thinner materials in the runners, leading to higher stresses. The power company Statkraft has experienced grave cracking in runner blades on several runners [1]. In Sauda, Norway, the power company Elkem experienced runner failure in the Sønnå Høy power plant ( $P=106\text{MW}$ ,  $H=540\text{m}$ ) after a short time of operation [2]. The power company TrønderEnergi experienced severe cracking in their replacement runner for the Driva plant ( $P=71\text{MW}$ ,  $H=570\text{m}$ ) after less than 12 hours of operation [3]. One of the causes for such failures are thought to be dynamic loads on the blades caused by pressure fluctuations in the runner, and the difficulties to accurately simulate these dynamic phenomena using computer tools [4-6]. One of the causes of these

phenomena is rotor-stator-interaction, and hence influencing the fatigue and lifetime of the runner [7, 8].

When Statkraft decided to refurbish Tokke power plant, a three-party pressure pulsation research project was initiated in parallel, together with Andritz and NTNU. The goal of the project was to contribute to the knowledge of the development of static and dynamic pressures in the entire turbine, by delivering extensive measurement data from the runners available. To investigate the onboard static and dynamic pressures, two model and two prototype runners were made accessible for onboard installation of pressure transducers. Both models were designed to fit in the 5,1:1 scale model of the existing spiral casing at Tokke power plant. One runner was designed by Andritz. The other was designed by NTNU, to be used as a reference runner for the test rig. Of the two prototype runners available, one was the original Kværner runner commissioned in 1961, the other was the replacement runner delivered by Andritz, commissioned in 2009.

The model tests were performed in the Waterpower Laboratory at The Norwegian University of Science and Technology (NTNU) in Norway, on both model runners [9]. Pressure was measured in the NTNU model, and both pressure and strain were measured in the Andritz model. After commissioning of the Andritz replacement runner at Tokke power plant, this runner was amongst others instrumented with onboard pressure transducers and strain gauges at the outlet of the runner blade. The common goal of the measurement described in this paper, was to acquire pressure and strain data from the prototype replacement runner just after commissioning was completed, to create foundation for the future analysis of the dynamics in the turbine. This knowledge will ultimately be used to discuss a possible scale-up relation between model and prototype.

Onboard pressure and strain measurements have been performed previously. This work has been focused on low head Francis turbines [5, 10-13]. The runners in this project are high head turbines. To the author's knowledge, such measurements have not been performed on both model and prototype for the same unit.

Measurements on both prototype runners were performed. In October 2008, the original runner on Unit 4 was instrumented and tested by NTNU and Statkraft alone. This was a Kværner runner with splitter blade design. After the test was completed and the logger retrieved, it was quickly discovered that the logger had been destroyed by water intrusion into the logging unit compartment. Hence, the test was a failure, and no data was obtained. In January and February 2009, the Andritz replacement runner on Unit 3 was instrumented and tested by all project participants. This test was performed successfully. The setup from this test and some preliminary results will be presented in the following. A retest of the failed Unit 4 test will probably be performed during the summer of 2010.

In the project, Statkraft provided funding for most of the costs, and access to the runners in question. Andritz also contributed to the funding and project organization.

NTNU and Andritz together took care of the instrumentation. NTNU performed the tests, and was assisted by Andritz on the Unit 3 test.

## 2. Methods

### *Description of logging chain*

To obtain measurement results to increase the understanding of the dynamic phenomena in the turbine, the prototype turbine with replacement runner was instrumented quite extensively. The authors wanted to measure the pressure and strain in the runner during operation. For the pressure measurements on the outlet of the runner blade, it was decided to use the same sensor as was used in the model runner tests, a Kulite LL080 strain gauge based miniature pressure transducer [9], equipped with over-pressure protection. These were placed in the same relative position as for outlet sensors on the model runners.

Three Kistler Type 7031 Quartz pressure sensors were integrated in the pressure side on the inlet of one blade. The positions of these were relatively the same as for the inlet sensors on the model turbines. This integration process was performed while the runner was still in the workshop.

For the strain measurements, 350 $\Omega$  strain gauges were placed at 16 different places on the runner blade outlet. Ten were placed in the radial direction, and 6 in tangential direction. Fourteen were placed on the suction side, 2 on the pressure side. All but two were placed on the same blade; the last two were placed on a neighboring blade, for reference.

The onboard prototype logging unit contained a National Instruments Compact Rio 9014 Real-Time controller, with an eight slot chassis. In this chassis, there were six NI 9237 strain gauge logging modules, receiving four channels of +/- 25mV signals. Two of the strain gauge modules were used for the Kulite outlet pressure transducers, and four modules for the strain gauges. There were also installed one NI 9239 +/- 10V logging module. This module acquired the voltage from the Kistler Type 5073 charge amplifier, which was receiving the signals from the Kistler Type 7031 sensor placed in the inlet pressure side. The system was powered by a 24V 13Ah battery pack. On the logging unit, bridge completions for the strain gauges were installed, and strain gauge calibration performed. The software was written in the NI LabView Real-Time language. This logging system enabled dynamic measurement of all onboard pressure sensors and strain gauges simultaneously. The system resolution was 24 bit, and the logging frequency was set to the prime number 1613Hz, reducing aliasing effects.

It was a desire to ensure stable operation of the logging unit by insuring stable temperature of the modules during each logging period. Due to this, the logging unit was turned on with voltage supplied to all components while the runner was filled with

water. By this, temperature gradients in the components during acquisitions were reduced.

The excitation voltage used for the NI 9237 modules was 3,3V. To reduce the current draw from the modules but still keeping excitation on for heating purposes, the excitation voltage was set to the lowest available voltage (2,5V) while the logger was inactive. Before each measurement sequence, the excitation was increased to 3,3V. This voltage ramp was also used as a reset signal for the Kistler charge amplifier.

In addition to the onboard measurement equipment, other sensors were logged using a second logging system. At three different places, Kulite XTE 190 pressure transducers were flush mounted in the lower cover, to measure the pressure in the rotational cavity. They measured the pressure after the guide vane outlet, and before the runner inlet, at three different angular positions relative to the guide vane axis. Two Druck PTX pressure transmitters were placed in the draft tube cone. An in-house key phaser was mounted on the shaft above the turbine radial bearing, and a measure of the guide vane servo stroke was established using an ASM wire potentiometer. All these channels were logged simultaneously, with the same logging frequency as for the onboard system.

Both systems were triggered by the same physical trigger, to be able to correlate the two systems in time. However, no key phaser was used on the onboard system. The stability of the two different logging unit clocks is not yet verified, so a correlation on a millisecond scale between the two systems will not be possible.

### *Description of mounting*

The pressure transducers were fixed on the blades using cyanoacrylate, as with the strain gauges. The pressure transducers were fixed in the same relative position on the prototype runner blades as for the model runners, see **Figure 1**. The strain gauges were fixed in positions such that the data would be suitable for comparison with FEM analysis. All cables from all onboard sensors were placed downstream the pressure sensors. Then all cables were covered with polyester, to create a smooth surface reducing the adverse effects of the hydraulic passage alteration. All cables were collected at the runner cone, where soldering tags were used as water stops. Then, the cables were lead through water tight holes into the watertight compartment housing the logger.

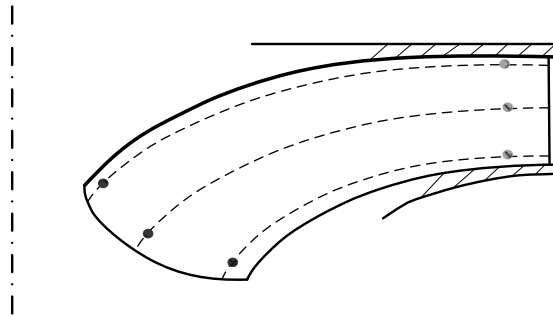


*Figure 1 - Placement of pressure transducers in prototype runner blade. Light grey markers indicate Kistler quartz sensors at the inlet, and dark markers indicate Kulite pressure transducers at the outlet.*



*Figure 2 - Strain gauges and pressure covering cables transducers with cables fixed, before covering*

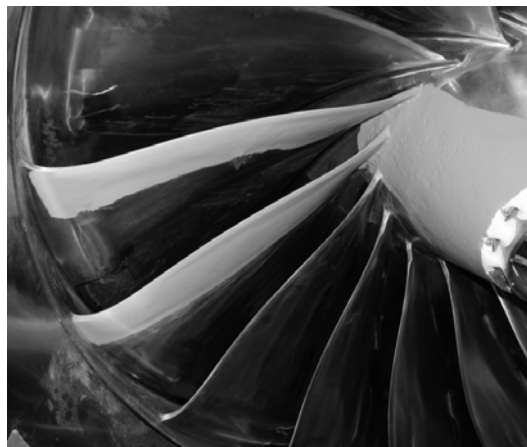


*Figure 3 - Runner after cables.*



*Figure 4 - Inlet pressure sensors during installation*

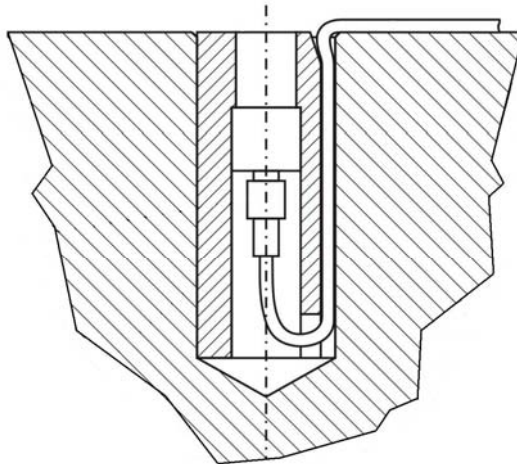


*Figure 5 - Sketch of inlet sensor lowered into the inlet of the blade*



For the inlet pressure sensors, the runner was modified in the Andritz workshop. Holes were drilled at the pressure side inlet to lower the Kistlers into the blade, see *Figure 4*. The sensors were fixed in a plexi glass housing, see *Figure 5*. The cables were also lowered into the blade, brought up through the upper part of the runner, under the labyrinth seals, and into the runner hub.

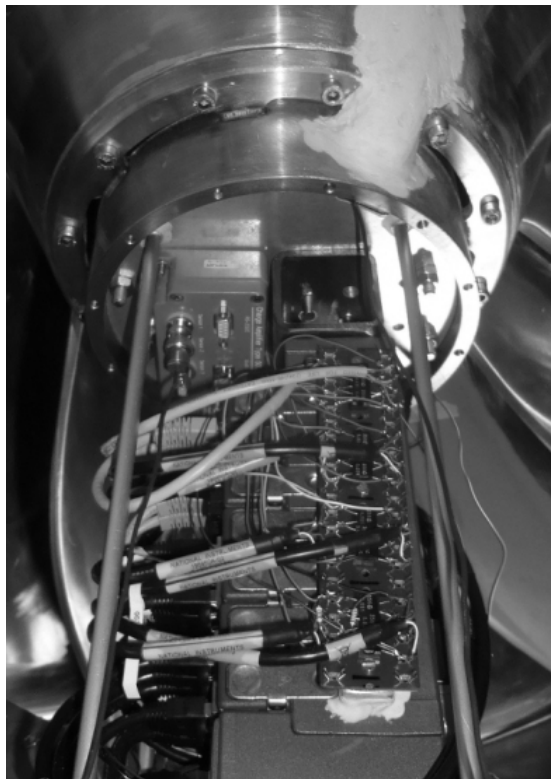


*Figure 6 - Installing the logging unit in the runner cone*

*Measurement sequence*

The software was written with the aim of both capturing the development of the measured properties during ramping transients, and stable operational points. For the stable points, pressure and strain were logged individually in time. However, there were also periods within each stable point where strain and pressure were measured simultaneously. This was done both to capture low frequency fluctuations (using longer logging periods on fewer channels), and the correlation between pressure and strain (all channels for a shorter time window). The built-in memory buffer was limited, so all channels could not be logged simultaneously for longer periods of time, without an approximately 80ms 'write-to-file-interruption'. The flow diagram that the software was derived from, enabled all these features (see *Figure 7*).

When all sensors were mounted and tested, the unit was filled. First, all channels were logged while the unit went from standstill to full speed no load. Then all sensors were logged during a slow 20% to 100% load increase, and then during a slow 100% to 20% load decrease. Then, 14 stable operating points were logged, including reference points. The total test period was of approximately 270 minutes.

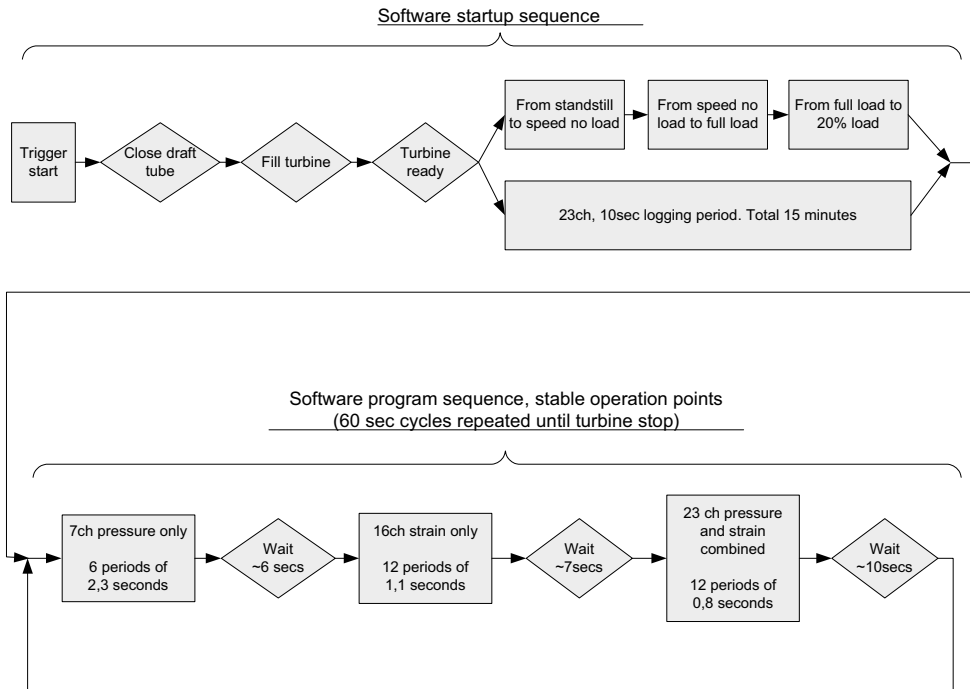


Figure 7 - Flow diagram for CompactRio onboard logging software

### 3. Results

The three Kistler quartz inlet pressure sensors were installed in the blade in the workshop. After commissioning, it was discovered that two of these had failed during the commissioning tests, but one was still functioning. This was discovered by checking the insulation resistances, which read too low values. Therefore, cable damage was a probable cause. After the measurement was finished, it was discovered that the last inlet Kistler also had failed. Also here, the insulation resistance was too low. The result was that no data was obtained from the inlet of the prototype.

After the measurement, it was also discovered that one of the six Kulite outlet sensors had failed (sensor number S-2). However, the remaining five had been functioning well during the entire test. All the strain gauges functioned well through the test.

In the following, relative mean values from the pressure measurement are presented. For description of sensor placement, see *Figure 1* and *Table 1*.

Sensor name	Outlet sensor position
P-1	Pressure side, crown side of blade
P-2	Pressure side, mid blade
P-3	Pressure side, band side of blade
S-1	Suction side, crown side of blade
S-2	Suction side, mid blade
S-3	Suction side, band side of blade

*Table 1 – Outlet Kulite transducer positions*

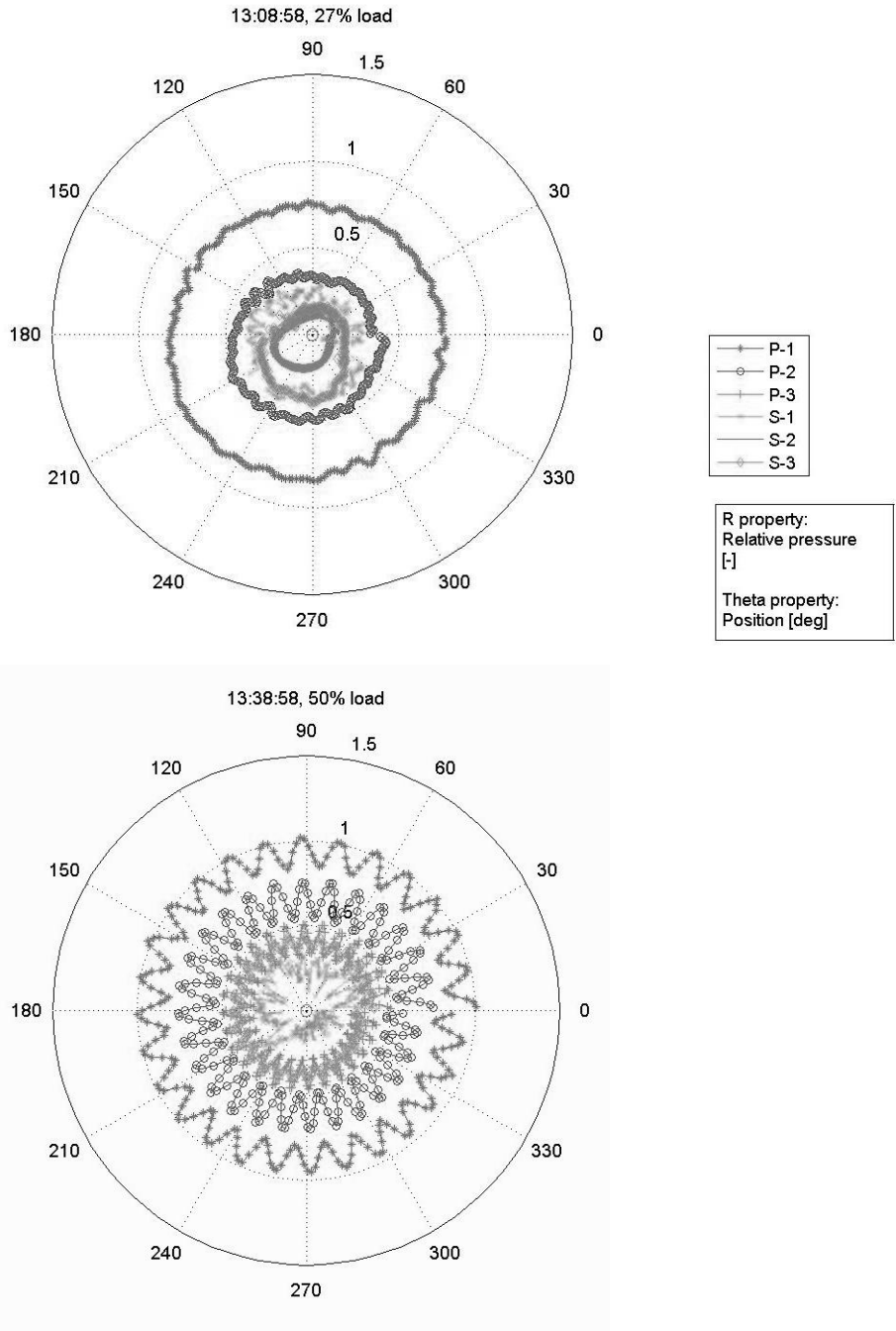


Figure 8 - Polar plot, outlet pressure at 27% and 50% load, one runner revolution.

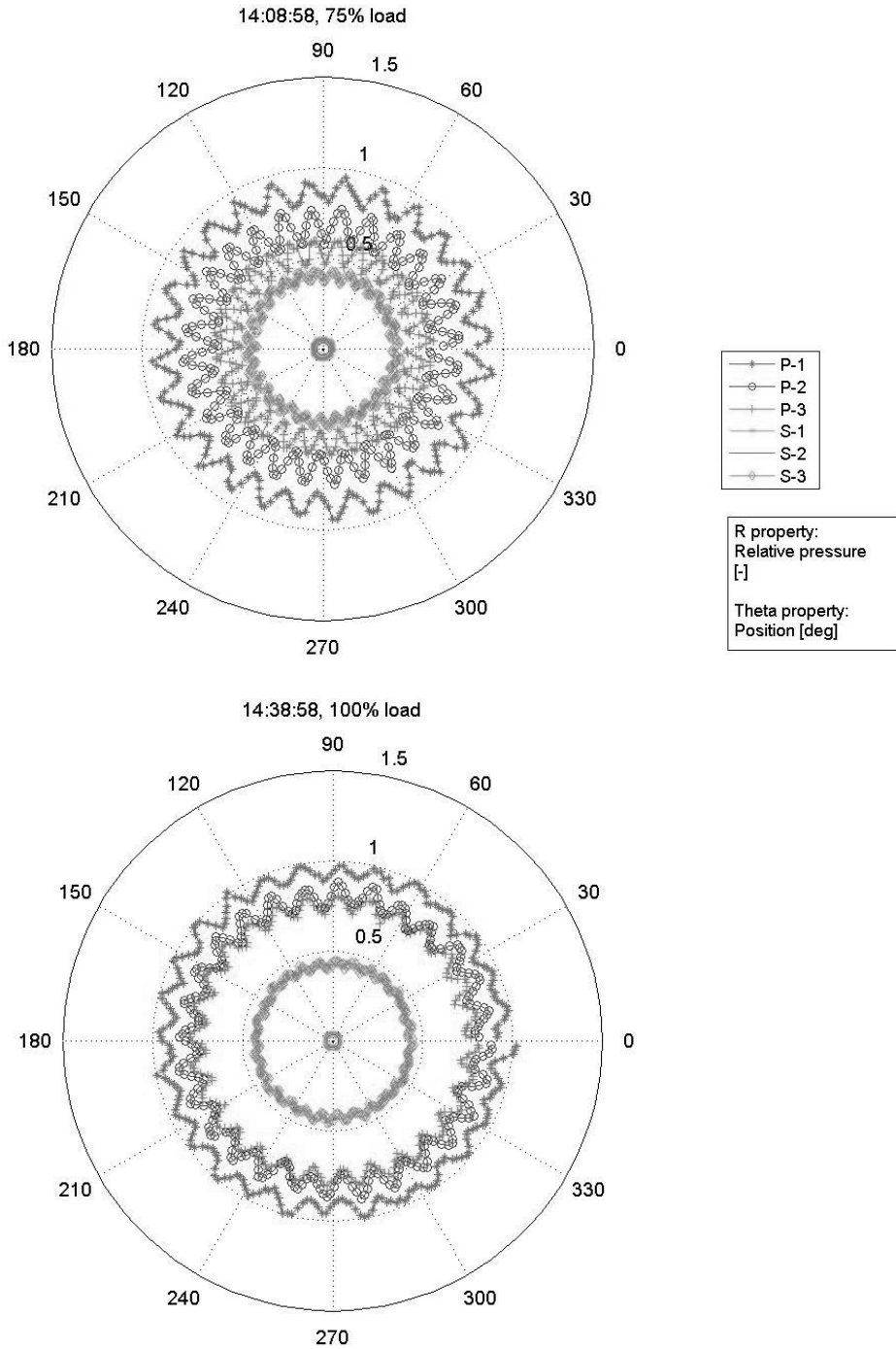


Figure 9 - Polar plot, outlet pressure at 75% and 100% load, one runner revolution

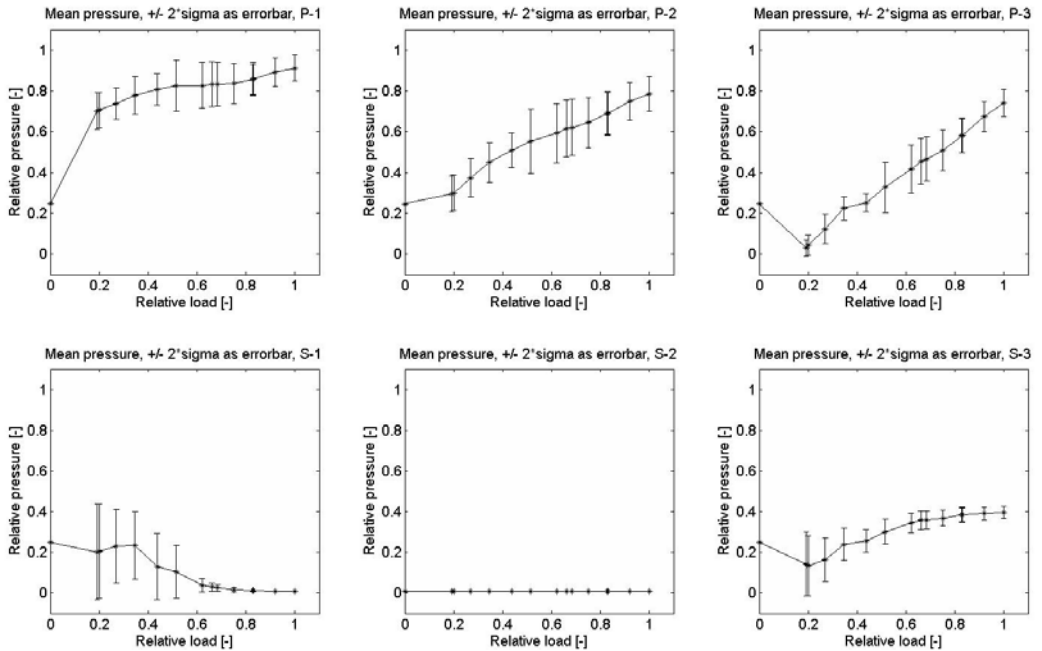


Figure 10 - Mean pressure from runner transducers over load range. The error bar is indicating  $\pm 2$  standard deviations of each steady operational point.

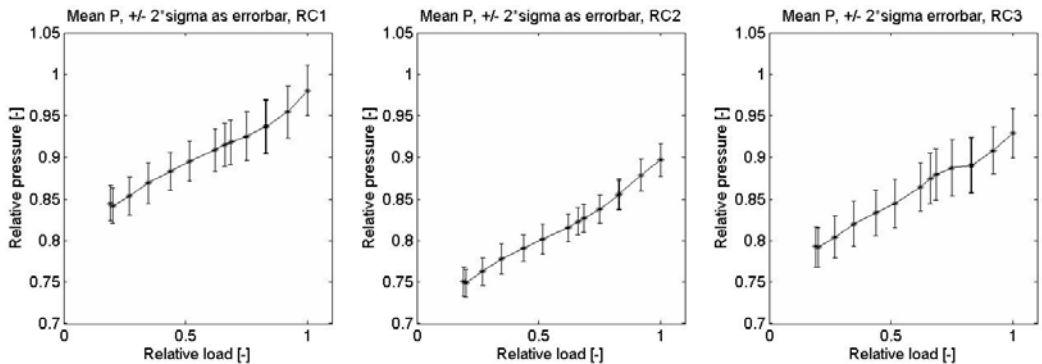


Figure 11 - Mean pressure from rotational cavity transducers over load range. The error bar is indicating  $\pm 2$  standard deviations of each steady operational point.

## 4. Discussion

### *Logging chain*

After the first failure, the logging equipment used proved to function well. There was however one downside. This was the onboard storage. Not being able to communicate with the logger during the test, there was no possibility to verify that the logger was actually running. To check that data had been stored, the turbine had to be stopped and emptied. One way to avoid this would have to use a wireless transmission system . This would require a hole in the shaft, running from the runner and through the bearings. The cables could have exited shaft above the bearing, to be connected to a transmitter. This would allow for real-time monitoring of the data logged. However, creating a hole in the shaft to allow for cables exiting the shaft was not considered an option.

### *Runner sensors*

In **Figure 8** and **Figure 9**, the relative pressure levels for one runner revolution are plotted. In Francis turbines, the blade passing frequency is one of the most dominant frequencies appearing. In **Figure 8**, one can see that at 27% load the blade passing frequency is quite dampened. This is due to the highly chaotic flow at this off design condition. When increasing the load to 50%, the blade passing is clearly visible as a smooth sine-like curve. At 75% and 100% in **Figure 9** one can also clearly see the blade passing; however, the amplitude seems to be a little dampened and influenced by noise compared to the 50% load point.

The pressure development in the runner through the load range, shown in **Figure 10**, is highly dependent on how the blade profile was designed. The U\*Cu distribution (**Figure 12**), force balancing etc is greatly affecting the flow. The authors will not reveal the design philosophy of the runner, so a detailed study of the pressure development must be omitted. The steady pressure level graphs will therefore be left uncommented. However, the error bars in **Figure 10** indicates the 95,45% confidence interval for the level of dynamic pressure fluctuations. These show a higher level of fluctuations in the region of 50 to 70% of full load, which is in accordance to what have been measured in the draft tube at several previous measurements.



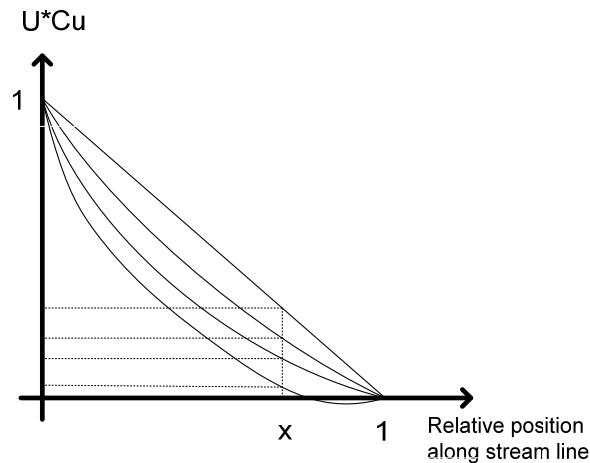


*Figure 12 - The chosen  $U*Cu$  distribution highly affects the pressure distribution in the hydraulic channel; hence the design philosophy is a key to commenting the measured pressure levels.*

One interesting result was obtained looking at the pressure on the outlet suction side, at the blade to crown junction. At first glance, it seemed like the sensor was damaged, because the pressure measured was very close to absolute zero. However, after full load ramps, the results repeated itself. Therefore, it seems like the pressure at this location approaches zero.

#### *Rotational Cavity*

From the **Figure 11**, it can be seen that the pressure after the guide vanes increase with load. According to Bernoulli, this should indicate that the velocity decrease. As the guide vanes opens, the area increases, and so does the flow. If the velocity actually decreases will be dependent on the guide vane profile, which will not be discussed here. However, according to Larsson [14], the pressure field and velocity distribution is highly dependent on the operational point. Larsson found significantly different static and dynamic pressures at different combinations of flow and rotational speeds.

Antonsen [15] concluded that the pressure distribution in the guide vane cascade is dependent on both the profiling of the guide vane and the opening. When the guide vanes are operated from lower to higher opening, pressure and suction side shifts, and the velocity profile changes accordingly. These properties depend on the design philosophy of the guide vane cascade. In addition to this, the pressure sensors mounted in the rotational cavity in the work presented in this paper, move relatively to the guide vane trailing edge as the load is changed. It is not a problem to calculate this relative movement, but when the geometry of the guide vane is confidential, the flow field will still be unknown. Based on the findings in [14] and [15], and the unknown design

philosophy of the guide vane profiles, the topic of rotational cavity pressure development will not be discussed thoroughly here.

The results and the discussion regarding the strain gauge measurements performed in this project will be presented at a later occasion.

## 5. Conclusion

The logging system developed proved to be a success. Hence, the measurement resulted in extensive measurement data from the Andritz replacement prototype. The measurement was expensive in both money and time, and such measurements will probably be performed at rare occasions. However, the obtained data will form a solid foundation for the future work.

Some relative pressure data have been presented. A more detailed study of the dynamics in the pressure and strain data is yet to be performed, and this analysis will be an integral part of the PhD project that carried out this measurement.

## 6. Future work

The future work includes several activities. A deeper study of the measurement data will be carried out. Here, frequency analyses of both model and prototype data will be performed, and compared with CFD calculations. The correlation between prototype pressure and strain will be investigated. Finally, the pressure data from the model and prototypes will be compared, to search for possible similarities that will be of interest in a scale up discussion.

## 7. Acknowledgements

Ole Gunnar Dahlhaug (NTNU), for inspiration and drive in the early project phase. Kjell-Tore Fjærvold (Statkraft), for funding, enthusiasm, support and facilitating the measurement.

Statkraft Region Øst and Kraftverksgruppe Tokke, for invaluable on-site assistance. Energibedriftenes Landsforening, [www.ebl.no](http://www.ebl.no), and Statkraft, for funding.

## 8. References

- 1 **Fjærvold, K.T.** Personal Communication regarding runner fatigue failures in Statkraft. In Kobro, E., ed Trondheim, 2009).
- 2 **Åril, B.** Sønnå Høy - Runner Breakdown (in Norwegian). *Produksjonsteknisk Konferanse* Gardermoen, 2009).
- 3 **TrønderEnergi.** Løpehjulet i Driva løper ikke lenger. *Lyspunktet* (TrønderEnergi, 2008).

- 4 Bjørndal, H.** The hunt for more effective units result in new problems (in Norwegian). *Produksjonsteknisk Konferanse Gardermoen*, 2009).
- 5 Avellan, F., Etter, S., Gummer, J.H. and Seidel, U.** Dynamic pressure measurements on a model turbine runner and their use in preventing runner fatigue failure *Proceedings of the XXIst IAHR Symposium on hydraulic machinery and systems, Lausanne*.
- 6 Sick, M., Michler, W., Weiss, T. and Keck, H.** Recent developments in the dynamic analysis of water turbines. *Journal of Power and Energy*, 2009, **223**(JPE578), 13.
- 7 Seidel, U. and Grosse, G.** New approaches to simulate the dynamic behaviour and dynamic stress of Francis and pump turbine runners *IAHR Int. Meeting of WG on Cavitation and Dynamic Problems in Hydraulic Machinery and Systems Barcelona*.
- 8 Vu, T.C. and B.Nennemann.** Modern trend of CFD application for hydraulic design procedure *23rd IAHR Symposium - Yokohama*.
- 9 Kobro, E., Dahlhaug, O.G. and Nielsen, T.** Onboard pressure Measurements in Francis Model Runner Blades. *24th IAHR Symposium on Hydraulic Machinery and Systems* (IAHR, Foz Do Iguazu, Brazil, 2008).
- 10 Lowys, P.Y., Doyon, J., Couston, M. and Vuillerod, G.** Dynamic behaviour of low head Francis turbines. *10th international meeting of the work group on the behaviour of hydraulic machinery under steady oscillatory conditions*, p. 9 Trondheim, Norway, 2001).
- 11 Farhat, M., Natal, S., Avellan, F., Paquet, F., Lowys, P. and Couston, M.** Onboard measurements of pressure and strain fluctuations in a model of low head Francis turbine. Part 1: Instrumentation *Proceedings of the XXIst IAHR Symposium on hydraulic machinery and systems, Lausanne*.
- 12 Lowys, P., Paquet, F., Couston, M., Farhat, M., Natal, S. and Avellan, F.** Onboard measurements of pressure and strain fluctuations in a model of low head Francis turbine. Part 2: Measurements and preliminary analysis results *Proceedings of the XXIst IAHR Symposium on hydraulic machinery and systems, Lausanne*.
- 13 Farhat, M., Avellan, F. and Seidel, U.** Pressure fluctuation measurements in hydro turbine models *The 9th International Symposium on Transport Phenomena and Dynamics of Rotating Machinery, Honolulu, Hawaii*.
- 14 Larsson, C.** Experimental and theoretical analysis of inlet flow of Francis Turbine Runner. *Department of Energy and Process Engineering* (Norwegian University of Science and Technology, Trondheim, 2003 ).
- 15 Antonsen, Ø.** Unsteady flow in wicket gate and runner with focus on static and dynamic load on runner. *Department of Energy and Process Engineering*, p. 86 (Norwegian University of Science and Technology, Trondheim, 2007).

## **PAPER 3**

*Kobro, E., Nielsen, T. K., and Dahlhaug, O. G., 2010, "Data Analysis from Onboard Francis Model Runner Pressure Measurements", The 13th International Symposium on Transport Phenomena and Dynamics of Rotating Machinery, Honolulu, Hawaii, USA.*

Is not included due to copyright

## **PAPER 4**

*Kobro, E., and Nielsen, T. K., 2010, "Analysis of Onboard Pressure and Strain Measurement Data from High Head Francis Prototype Runner, and Discussion on Runner Lifetime", Journal of Fluids Engineering (paper under review, submitted on February 24<sup>th</sup>, 2010)*

Is not included due to copyright